

# Transformers Provably Learn to Internalize Chain-of-Thought

Yixiao Huang<sup>1†</sup>   Hanlin Zhu<sup>1</sup>   Zixuan Wang<sup>2</sup>  
Jiantao Jiao<sup>1</sup>   Stuart Russell<sup>1</sup>   Somayeh Sojoudi<sup>1</sup>   Song Mei<sup>1</sup>

<sup>1</sup>UC Berkeley   <sup>2</sup>Princeton University

## Abstract

Chain-of-Thought (CoT) prompting substantially improves the sample efficiency of transformers, reducing the complexity of tasks like parity learning from exponential to polynomial in the input length. However, generating explicit reasoning steps at inference is computationally expensive. Implicit Chain-of-Thought (ICoT) has emerged as a promising empirical remedy that trains models to internalize intermediate steps within their hidden states, but its theoretical foundations remain poorly understood. We give the first theoretical analysis of ICoT, proving that an  $L$ -layer transformer trained under our proposed Log-ICoT curriculum learns  $k$ -parity with  $\text{poly}(n)$  samples and  $L = \log_2 k$  training stages. This matches the sample efficiency of explicit CoT while eliminating its inference overhead, and extends prior one-layer parity guarantees to multi-layer architectures. Compared to standard ICoT, which removes thinking tokens one at a time, Log-ICoT removes them in geometric chunks, reducing the number of stages from linear in  $k$  to logarithmic. Experiments on multi-layer transformers confirm the theory and visualize how reasoning is progressively absorbed into deeper layers.

## 1 Introduction

Chain-of-Thought (CoT) reasoning [Wei et al., 2022] has become a cornerstone for enabling Large Language Models (LLMs) to solve challenging tasks. By generating explicit intermediate tokens, CoT decomposes complex problems into manageable sub-steps, significantly boosting performance. However, this reasoning power comes at a high cost: the explicit generation of thinking tokens substantially increases inference latency and computational overhead.

To address this, Implicit CoT (ICoT) [Deng et al., 2024] has emerged as a promising paradigm. ICoT trains models to internalize reasoning steps within their hidden states by progressively removing intermediate steps during fine-tuning, eliminating the need for explicit token generation at inference time. Despite promising empirical evidence, the underlying mechanics of when and how models internalize these steps remain poorly understood. Furthermore, the standard ICoT curriculum, which removes intermediate steps one by one, scales linearly with the length of the reasoning chain, leading to inefficient training.

**Parity learning as a testbed.** We study these questions in the setting of  $k$ -parity learning, a classic problem that has emerged as a canonical testbed for the role of intermediate supervision in transformer training [Kim and Suzuki, 2024, Wen et al., 2024, Li et al., 2026]. The task is provably hard for finite-precision gradient-based methods without intermediate supervision: any algorithm using  $\text{poly}(n)$  samples and queries cannot achieve non-trivial accuracy [Shalev-Shwartz et al., 2017,

---

<sup>†</sup>Correspondence: yixiaoh@berkeley.edu

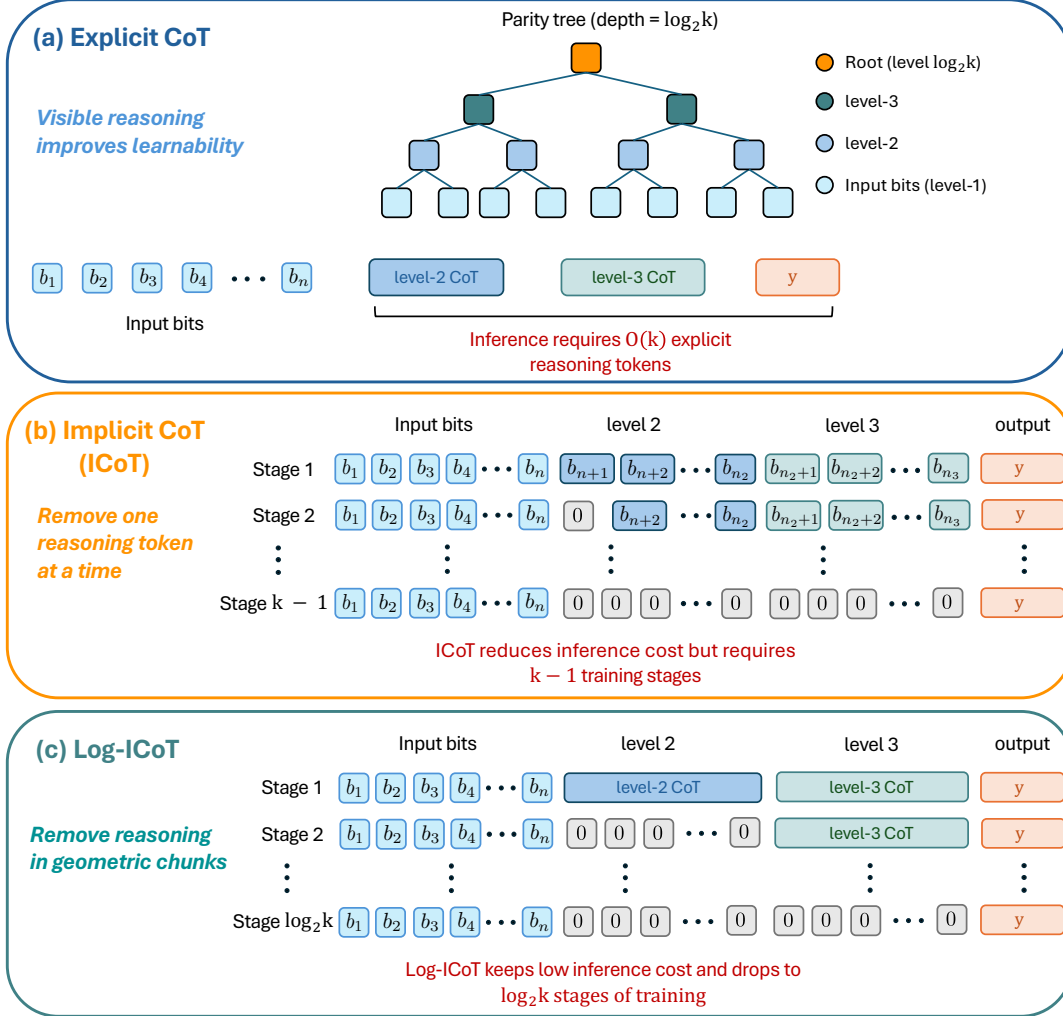


Figure 1: **Comparison of training paradigms on the  $k$ -parity task.** (a) Explicit CoT supervises every node of the parity tree, achieving sample-efficient learning at the cost of  $\Omega(k)$  sequential reasoning tokens at inference. (b) Implicit CoT (ICoT) [Deng et al., 2024] internalizes reasoning into hidden states by removing intermediate tokens one at a time, eliminating the inference cost but requiring  $k - 1$  training stages. (c) Our Log-ICoT curriculum removes tokens in geometric chunks aligned with the parity tree’s levels, reducing the number of training stages to  $\log_2 k$  while preserving inference efficiency.

Wies et al., 2022, Kim and Suzuki, 2024]. With explicit CoT supervision, however, even one-layer transformers can learn to solve parity efficiently [Kim and Suzuki, 2024, Wen et al., 2024]. This makes parity an ideal task for studying how CoT reshapes optimization to make expressible solutions reachable, and how ICoT preserves this advantage while eliminating the inference-time cost of explicit reasoning.

**Our contributions.** We present the first theoretical analysis of ICoT, establishing that the sample efficiency of explicit CoT can be preserved when reasoning is internalized into hidden states. Specifically:

- **Log-ICoT curriculum.** We introduce Log-ICoT, a new ICoT curriculum that removes intermediate CoT steps in geometric increments matching the parity tree’s recursive structure

(Figure 1). Compared to the linear-stage curriculum of standard ICoT [Deng et al., 2024], Log-ICoT requires only  $L = \log_2 k$  training stages.

- **Convergence guarantee for multi-layer ICoT.** In Theorem 1, we prove that an  $L$ -layer transformer trained under Log-ICoT solves  $k$ -parity with  $\text{poly}(n)$  samples and  $\log_2 k$  gradient updates, matching the sample complexity of explicit CoT [Kim and Suzuki, 2024, Wen et al., 2024] while producing the answer in a single forward pass at inference (vs.  $O(k)$  sequential steps for autoregressive CoT generation). This extends prior parity guarantees from one-layer to multi-layer architectures.
- **Resolving multi-layer training challenges.** Our analysis identifies two key challenges in analyzing the training dynamics of multi-layer transformers and resolves them via three design choices: *gated connections* [Srivastava et al., 2015] to prevent representation collapse across layers, a *customized causal attention mask* and *integer quantization* of attention weights combined with a stage-wise learning rate to control error propagation across training stages.
- **Empirical verification.** We verify our theoretical findings through numerical experiments on a multi-layer transformer (Section 4).

## 1.1 Related Work

**Chain-of-thought and its variants.** Chain-of-thought (CoT) [Wei et al., 2022] can enhance LLMs’ reasoning capabilities by letting models output the intermediate thought tokens. It can be encouraged only in the prompt [Khot et al., 2022, Zhou et al., 2022] or be included in the training set [Yue et al., 2023, Yu et al., 2023, Wang et al., 2023a, Shao et al., 2024]. A line of theoretical works also study the advantages of the CoT method via expressivity [Liu et al., 2022, Feng et al., 2023, Merrill and Sabharwal, 2023, Li et al., 2024b] or training dynamics [Zhu et al., 2024b, Wen et al., 2024, Kim and Suzuki, 2024]. A more recent line of work studies variants of CoT to improve the model performance or reduce the inference cost, including ICoT [Deng et al., 2023, 2024], pause tokens [Goyal et al., 2023], filler tokens [Pfau et al., 2024], planning tokens [Wang et al., 2023b], token assorted [Su et al., 2025], chain of continuous thought [Hao et al., 2024], etc. Compared to CoT, its variants are much less explored, especially theoretically. London and Kanade [2025] theoretically show that the pause token can increase expressivity, and Zhu et al. [2025a,b], Gozeten et al. [2025] theoretically show the advantage of continuous CoT. Our paper contributes to the field by providing the first theoretical results demonstrating the advantage of the ICoT method, i.e., it can bridge the gap between expressivity and learnability.

**Training dynamics of transformers.** There is a very rich line of literature studying the optimization of transformer-based models [Jelassi et al., 2022, Bietti et al., 2023, Mahankali et al., 2023, Fu et al., 2023, Zhang et al., 2024, Li et al., 2024a, Huang et al., 2024, Ildiz et al., 2024]. Many works focus on how certain attention patterns are formed during training [Tian et al., 2023a,b, Guo et al., 2024]. Another line of work focuses on various reasoning abilities or patterns of transformers through the lens of training dynamics [Boix-Adsera et al., 2023, Nichani et al., 2024, Wang et al., 2024, Ren et al., 2024, Zhu et al., 2024b, Guo et al., 2025, Huang et al., 2025a, Chen et al., 2024, Huang et al., 2025b, Ma et al., 2026]. The most related works to our setting are Wen et al. [2024], Kim and Suzuki [2024], which show that CoT enables much better sample efficiency when learning parity functions with secret indices. Our work follows the setting of Kim and Suzuki [2024] and takes a further step to study the sample complexity of ICoT via training dynamics. Our work shows that ICoT enjoys both sample efficiency and low inference-time cost. Moreover, we provide an end-to-end

analysis on multi-layer transformers, which is more practical and challenging than the one-layer transformer considered in [Wen et al. \[2024\]](#), [Kim and Suzuki \[2024\]](#). Our analysis also builds on [Wang et al. \[2025\]](#), who studied attention-only multi-layer transformers. In contrast, the link function in our setting introduces additional cross-layer noise, which we suppress via gated connections.

## 2 Preliminaries

**Notations.** For any integer  $N > 0$ ,  $[N] := \{1, 2, \dots, N\}$ . We use lower-case and upper-case bold letters (e.g.,  $\mathbf{a}$ ,  $\mathbf{A}$ ) for vectors and matrices. Let  $\mathbf{e}_{d,i} \in \mathbb{R}^d$  denote the standard basis vector with a 1 in the  $i$ -th coordinate and  $\mathbf{I}_K \in \mathbb{R}^{K \times K}$  the identity. The multi-linear inner product of vectors  $\mathbf{x}_1, \dots, \mathbf{x}_r \in \mathbb{R}^d$  is defined as

$$\langle \mathbf{x}_1, \dots, \mathbf{x}_r \rangle := \sum_{i=1}^d \prod_{j=1}^r x_{j,i},$$

which generalizes the standard inner product:  $\langle \mathbf{x}_1 \rangle = \mathbf{x}_1^\top \mathbf{1}_d$  and  $\langle \mathbf{x}_1, \mathbf{x}_2 \rangle = \mathbf{x}_1^\top \mathbf{x}_2$ . Let  $q : \mathbb{R} \rightarrow \mathbb{Z}$  denote nearest-integer rounding and extend  $q$  entrywise to matrices.

### 2.1 Task Settings

Assume  $n \geq k \geq 2$  with  $k = \Theta(n)$ , and let  $\mathcal{S}$  denote the set of all size- $k$  subsets of  $[n]$ . Following [Kim and Suzuki \[2024\]](#), [Wen et al. \[2024\]](#), we consider the  $k$ -parity problem: given a secret index set  $S \sim \text{Unif}(\mathcal{S})$  and an input  $\mathbf{b} \sim \text{Unif}(\{\pm 1\}^n)$ , the label is the parity  $y = p_S(\mathbf{b}) := \prod_{j \in S} b_j$ . Here  $n$  is the input length and  $k = |S|$  controls task hardness. We work in the finite-sample setting with a dataset of  $B$  i.i.d. samples  $\{(\mathbf{b}^i, y^i)\}_{i=1}^B$ .

**Task decomposition.** We assume  $k = 2^L$  for an integer  $L$  and decompose the problem into a hierarchy of two-parities (Figure 1). The task forms a complete binary tree of height  $L$  with  $2k - 1$  total nodes. Leaf nodes at level 1 represent the input bits  $\{b_j : j \in S\}$  in the secret set  $S$ , and the  $k - 1$  internal nodes are indexed  $b_{n+1}, \dots, b_{n+k-1}$  from bottom to top, left to right. We write  $n_\ell := n + k(1 - 2^{-(\ell-1)})$  for the maximum index at level  $\ell$  (so  $n_1 = n$  and  $n_{L+1} = T := n + k - 1$ ). For each position  $j \in [T]$ , let  $p[j]$  be its parent in the parity tree if it exists, and set  $p[j] = \emptyset$  otherwise. For each internal node  $b_m$  ( $m > n$ ), let  $c_1[m], c_2[m]$  denote its two children with  $c_1[m] < c_2[m] < m$ . Set  $h[j] = 1$  for  $j \leq n$ , and define  $h[m]$  for  $m > n$  by  $n_{h[m]-1} < m \leq n_{h[m]}$ . The recursive parity relation  $b_m = b_{c_1[m]} \cdot b_{c_2[m]}$  holds at every internal node, and the root  $b_T$  equals the target  $y$ . A concrete construction of the parity tree is given in Figure 4 of Section B.1.

**Loss and oracle.** Let  $f_\theta : \{\pm 1\}^n \rightarrow \mathbb{R}$  be a differentiable parametrized model. We consider the empirical squared loss

$$\mathcal{L}_B(\theta) := \frac{1}{2B} \sum_{i=1}^B (y^i - f_\theta(\mathbf{b}^i))^2,$$

and evaluate performance by the population  $L_2$  error

$$\mathcal{E}(\theta) := \mathbb{E}_{S, \mathbf{b}} [(p_S(\mathbf{b}) - f_\theta(\mathbf{b}))^2].$$

An  $\varepsilon$ -approximate gradient oracle for  $\mathcal{L}_B$  is a (possibly randomized) map  $\tilde{\nabla} \mathcal{L}_B$  satisfying  $\|\tilde{\nabla} \mathcal{L}_B(\theta) - \nabla \mathcal{L}_B(\theta)\|_2 \leq \varepsilon$  for all queried  $\theta$ .

**Proposition 1** (Kim and Suzuki [2024], Theorem 2). *Suppose  $B = \Omega(n^\nu)$  and  $\|\nabla f_\theta\| = O(n^{\nu_1})$ . Then there exists an  $O(n^{-\nu_2})$ -accurate gradient oracle  $\tilde{\nabla}$  such that, with probability at least  $1 - \exp(-\Omega(n))$  over the random sampling, the output  $\theta(\mathcal{A})$  of any iterative algorithm  $\mathcal{A}$  making at most  $O(n^{\nu_3})$  queries to  $\tilde{\nabla}\mathcal{L}_B$  satisfies  $\mathcal{E}(\theta(\mathcal{A})) \geq 1 - O(n^{-\nu_4})$ , where  $\nu = 4\nu_1 + 4\nu_2 + 2\nu_3 + 2\nu_4 + 1$ .*

## 2.2 Model

**Architecture.** We consider an  $L$ -layer simplified transformer following Wang et al. [2025]. To process the entire dataset in parallel, we stack the  $j$ -th bit across all  $B$  samples into a vector  $\mathbf{b}_j = (b_j^1, \dots, b_j^B)^\top \in \mathbb{R}^B$ , so the input data  $\mathbf{D} = [\mathbf{b}_1, \dots, \mathbf{b}_T] \in \mathbb{R}^{B \times T}$  is processed as a single batch using a shared positional encoding.

**Embedding layer.** We set  $T := n + k - 1$  and embedding dimension  $d := T + B(L + 1)$ . For each  $j \in [T]$ , the embedding is

$$\mathbf{x}_j = \mathbf{E}(\mathbf{D})_j = \begin{bmatrix} \mathbf{p}_j \\ \mathbf{b}_j \\ \mathbf{0}_{B \cdot L} \end{bmatrix} \in \mathbb{R}^d,$$

where  $\mathbf{p}_j := \mathbf{e}_{T,j} \in \mathbb{R}^T$  is a one-hot positional encoding and the final  $B \cdot L$  dimensions are reserved for the residual stream [Elhage et al., 2021].

**Attention layer.** We use a single-head attention per layer, reparameterizing the key-query matrix as  $\mathbf{W}_{\text{KQ}} := \mathbf{W}_{\text{K}}\mathbf{W}_{\text{Q}}^\top$  following Tian et al. [2023a], Zhu et al. [2024b], Li et al. [2024a]. We optimize only the upper  $T \times T$  block  $\mathbf{W} \in \mathbb{R}^{T \times T}$ , fixing other entries to zero so that attention scores depend only on positional encodings. The value matrix is the identity:

$$\mathbf{W}_{\text{KQ}} = \begin{bmatrix} \mathbf{W} & \mathbf{0}_{T \times B_L} \\ \mathbf{0}_{B_L \times T} & \mathbf{0}_{B_L \times B_L} \end{bmatrix}, \quad \mathbf{W}_{\text{V}} = \mathbf{I}_d, \quad B_L := B(L + 1).$$

**Definition 1** (Causal Self-Attention). *Given  $\mathbf{W} \in \mathbb{R}^{T \times T}$ , the causal self-attention module  $\text{Attn}(\cdot; \mathbf{W}) : \mathbb{R}^{d \times T} \rightarrow \mathbb{R}^{d \times T}$  is*

$$\text{Attn}(\mathbf{X}; \mathbf{W}) = \mathbf{X} \cdot \mathbb{S}(\mathbf{X}^\top \mathbf{W}_{\text{KQ}} \mathbf{X} + C),$$

where  $\mathbb{S}(\cdot)$  is the column-wise softmax and  $C \in \mathbb{R}^{T \times T}$  is the level-restricted causal mask

$$C_{j,m} = \begin{cases} 0 & \text{if } m \leq n \text{ and } j < m, \\ 0 & \text{if } m > n \text{ and } j \leq n_{h[m]-1}, \\ -\infty & \text{otherwise.} \end{cases}$$

A detailed discussion of the causal mask is provided in Section 3.2

**MLP layer.** The MLP layer applies a fixed link function  $\phi : [-1, 1] \rightarrow [-1, 1]$  pointwise.

**Definition 2** (Link function). *Following Kim and Suzuki [2024],  $\phi$  is symmetric and satisfies  $\phi(0) = -1$ ,  $\phi(\pm 1) = 1$ , so that  $\phi(\frac{a+b}{2}) = ab$  for  $a, b \in \{\pm 1\}$ . We further assume  $\phi$  is sufficiently smooth with  $\phi'(0) = \phi'(\pm 1) = 0$ , allowing the local Taylor expansion  $\phi(t) = -1 + ct^2 + O(|t|^4)$  and  $\phi'(t) = 2ct + O(|t|^3)$  around 0 for some constant  $c > 0$ .*

**Gated connections.** We use gated connections [Srivastava et al., 2015] as a structured alternative to standard residual connections. Conventional residual updates can suffer a trade-off between representation collapse and gradient vanishing [Xie et al., 2023, Zhu et al., 2024a], and several variants modify the residual pathway to resolve this, including ResiDual [Xie et al., 2023] and hyper-connections [Zhu et al., 2024a], both of which expand the residual stream into multiple parallel paths. We instead use a *position-wise* gated connection in the spirit of GTrXL [Parisotto et al., 2020], where each layer  $\ell$  has a gate vector  $\mathbf{g}^{(\ell)} \in \mathbb{R}^T$  controlling how the layer mixes the block update with the existing representation at each token position:

$$\text{GC}(\mathbf{A}, \mathbf{B}; \mathbf{g}) := \mathbf{A} \text{diag}(\mathbf{g}) + \mathbf{B}(\mathbf{I}_T - \text{diag}(\mathbf{g})).$$

**Definition 3** (Multi-layer Transformer). *Let  $L$  be the depth. The trainable parameters are  $\boldsymbol{\theta} := \{\mathbf{W}^{(\ell)}\}_{\ell \in [L]}$ . Initializing  $\mathbf{X}^{(0)} = \mathbf{E}(\mathbf{D}) \in \mathbb{R}^{d \times T}$ , the layer update is*

$$\mathbf{X}^{(\ell)} = \mathbf{X}^{(\ell-1)} + \mathbf{W}_O^{(\ell)} \text{GC}\left(\phi(\text{Attn}(\mathbf{X}^{(\ell-1)}; \mathbf{W}^{(\ell)})), \mathbf{X}^{(\ell-1)}; \mathbf{g}^{(\ell)}\right), \quad \ell \in [L].$$

The network output is  $\mathcal{T}_\theta(\mathbf{D}) = \mathbf{X}^{(L)}$ . For  $m \in [T]$ , the output at position  $m$  is

$$\mathcal{T}_\theta(\mathbf{D})_m = \mathbf{x}_m + \sum_{\ell=1}^L \mathbf{W}_O^{(\ell)} \left( g_m^{(\ell)} \phi\left(\sum_{j=1}^{m-1} \sigma_j(\mathbf{w}_m^{(\ell)}) \mathbf{x}_j^{(\ell-1)}\right) + (1 - g_m^{(\ell)}) \mathbf{x}_m^{(\ell-1)} \right),$$

where  $w_{j,m}^{(\ell)} = \mathbf{p}_j^\top \mathbf{W}^{(\ell)} \mathbf{p}_m$ , and  $\sigma_j(\mathbf{w}_m^{(\ell)})$  is the corresponding attention score. The readout layer  $\Psi_\ell \in \mathbb{R}^{d \times B}$  decodes the output as  $f_\theta^{(\ell)}(\mathbf{D}) = \Psi_\ell^\top \mathcal{T}_\theta(\mathbf{D})$ .

**Block-shift output and readout.** We fix  $\mathbf{W}_O^{(\ell)}$  as a block-shift operator that moves content from residual block  $[\ell]$  to block  $[\ell + 1]$ :

$$\mathbf{W}_O^{(\ell)} = \begin{bmatrix} \mathbf{0}_{T \times T} & \mathbf{0}_{T \times B_L} \\ \mathbf{0}_{B_L \times T} & \mathbf{e}_{L+1, \ell+1} \mathbf{e}_{L+1, \ell}^\top \otimes \mathbf{I}_B \end{bmatrix},$$

and the readout  $\Psi_\ell$  as a selector for block  $[\ell + 1]$ :

$$\Psi_\ell = \begin{bmatrix} \mathbf{0}_{T \times B} \\ \mathbf{e}_{L+1, \ell+1} \otimes \mathbf{I}_B \end{bmatrix}.$$

With this construction,  $\Psi_{\ell'}^\top \mathbf{W}_O^{(\ell)}$  is non-zero iff  $\ell = \ell'$ , so the readout at stage  $\ell$  extracts exactly the content written by layer  $\ell$ . By Lemma 10, gradients at well-trained layers are exponentially small, so we can focus on training one layer per stage.

## 3 Theoretical Results

### 3.1 Training Scheme

**Chain-of-Thought (CoT) for parity.** The parity tree described in Section 2.1 gives a natural sequence of intermediate computations. We expand the input vector  $\mathbf{b} \in \{\pm 1\}^n$  to a length- $T$  sequence  $\mathbf{b} \in \{\pm 1\}^T$  by appending the internal node values  $\mathbf{b}_{n+1}, \dots, \mathbf{b}_T$ , where each  $\mathbf{b}_m$  ( $m > n$ ) is computed via the recursion  $\mathbf{b}_m = \mathbf{b}_{c_1[m]} \cdot \mathbf{b}_{c_2[m]}$ . The CoT supervision trains the model to predict each  $\mathbf{b}_m$  at position  $m$  [Kim and Suzuki, 2024, Wen et al., 2024].

**Implicit Chain-of-Thought (ICoT).** ICoT [Deng et al., 2024] progressively removes intermediate CoT steps during training, internalizing the reasoning into hidden states so that at inference the model produces the answer directly without explicit reasoning. In the original formulation, removed CoT steps shorten the sequence. We instead pad with zeros, keeping the length fixed at  $T$ . This does not sacrifice inference efficiency, since the model still produces the answer in a single forward pass. This design is theoretically grounded by Merrill and Sabharwal [2026], who show that padding tokens expand transformer expressivity by serving as extra parallel scratch positions for intermediate computation. Concretely, each parity-tree level is computed in parallel across positions with one level per transformer layer. This contrasts with autoregressive CoT generation, which would require  $O(k)$  sequential steps.

**Log-ICoT curriculum.** We adopt a Log-ICoT curriculum as in Figure 1 (c) that removes CoT steps in *geometric increments*, mirroring the parity tree’s level structure:

- Stage 1: Full CoT (all positions  $\mathbf{b}_{n+1}, \dots, \mathbf{b}_T$  shown).
- Stage  $t$  ( $2 \leq t \leq L$ ): Replace positions  $\mathbf{b}_{n+1}, \dots, \mathbf{b}_{n_t}$  with padding (zeros), keeping  $\mathbf{b}_{n_t+1}, \dots, \mathbf{b}_T$  shown.
- Stage  $L$ : All CoT steps except the final output are padded.

Since  $L = \log_2 k$ , the curriculum contains only a logarithmic number of stages, in contrast to the linear number used in standard ICoT [Deng et al., 2024].

**Loss function.** At stage  $t$ , we use the squared loss summed over the predicted positions:

$$\mathcal{L}^{(t)}(\boldsymbol{\theta}) = \frac{1}{2B} \sum_{m=n_t+1}^T \|\Psi_t^\top \mathcal{T}_\theta(\mathbf{D})_m - \mathbf{b}_m\|^2. \quad (1)$$

This can be equivalently written as

$$\mathcal{L}^{(t)}(\boldsymbol{\theta}) = \frac{1}{2B} \sum_{i=1}^B \|\bar{\mathbf{y}}^i - f_\theta^\circ(\mathbf{b}^i)\|^2,$$

where  $\bar{\mathbf{y}}^i = (b_{n_t+1}^i, \dots, b_T^i)^\top$  collects the predicted positions for sample  $i$  and  $f_\theta^\circ(\mathbf{b}^i)_m = (\Psi_t^\top \mathcal{T}_\theta(\mathbf{D})_m)_i$ . This recovers the abstract form of Proposition 1 with a vector-valued predictor  $f_\theta^\circ : \{\pm 1\}^n \rightarrow \mathbb{R}^{T-n_t}$ .

**Algorithm.** At each stage  $t$ , we draw an independent fresh batch of size  $B$  and take one gradient step on  $\mathcal{L}^{(t)}$ , followed by integer quantization (Algorithm 1). Training proceeds sequentially through all  $L = \log_2 k$  stages. Thus  $B$  denotes the per-stage batch size. Since fresh samples are used at each stage, the total number of training samples used by the curriculum is  $BL = O(B \log k)$ .

**Evaluation.** At test time, we use the Stage  $L$  inference setup: random input bits filled in for positions  $1, \dots, n$ , and zeros for the remaining  $T - n = k - 1$  CoT positions. Concretely, given an independent test batch  $\mathbf{D}_{\text{test}} = [\mathbf{b}_1, \dots, \mathbf{b}_n, \mathbf{0}, \dots, \mathbf{0}] \in \mathbb{R}^{B \times T}$  with  $\mathbf{b}_j \sim \text{Unif}(\{\pm 1\}^B)$ , the target is  $(\mathbf{y}_{\text{test}})_i = \prod_{j \in S} b_j^i$  for  $i \in [B]$ . Performance is measured by the population  $L_2$  error  $\mathcal{E}(\theta)$ .

### 3.2 Key Challenges

There are two primary challenges in training multi-layer transformers. We discuss them in turn.

---

**Algorithm 1** Training Algorithm (Log-ICoT Curriculum)

---

**Require:** Per-stage batch size  $B$ , learning rate  $\eta_t = K_n n_t^2 / (2c)$

- 1: Initialize  $\mathbf{W}^{(\ell)}(0) = \mathbf{0}_{T \times T}$  for all  $\ell \in [L]$ ,  $\boldsymbol{\theta} := \{\mathbf{W}^{(\ell)}\}_{\ell \in [L]}$
  - 2: **for**  $t = 1, \dots, L$  **do**
  - 3:     Draw an independent fresh batch of  $B$  samples and construct the stage- $t$  padded CoT data.
  - 4:      $\boldsymbol{\theta}(t) \leftarrow q\left(\boldsymbol{\theta}(t-1) - \eta \tilde{\nabla}_{\boldsymbol{\theta}} \mathcal{L}^{(t)}(\boldsymbol{\theta}(t-1))\right)$
  - 5: **end for**
  - 6: **return**  $\hat{\boldsymbol{\theta}} = \{\mathbf{W}^{(\ell)}(L)\}_{\ell=1}^L$
- 

**Representation Collapse.** First, the input states collapse to a near-uniform value in late layers, causing the gradient to lose the ability to distinguish between token positions. For brevity, we drop the layer superscript in the following lemma. The result applies to any attention layer with weight matrix  $\mathbf{W}$ .

**Lemma 1** (Representation collapse of input states). *For  $B = \text{poly}(n)$ , with probability  $1 - \exp(-n^{\epsilon/16})$  over random sampling of the input data  $\mathbf{b}_1, \dots, \mathbf{b}_n$ , it holds that, for all  $n^{\epsilon/8} \leq m \leq n$ :*

$$\left\| \phi\left(\frac{1}{m-1} \sum_{\alpha \in [m-1]} \mathbf{b}_\alpha\right) + \mathbf{1}_B \right\|_\infty \leq O(n^{-\epsilon/16}).$$

*In particular, when  $\mathbf{W}$  is  $\mathbf{0}_{T \times T}$ , for all  $n^{\epsilon/8} \leq m \leq n$ , we have*

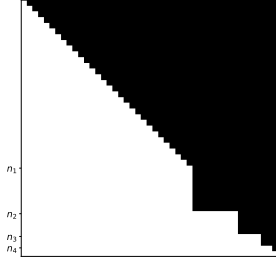
$$\left\| \phi\left(\sum_{j=1}^{m-1} \sigma_j(\mathbf{w}_m) \mathbf{b}_j\right) + \mathbf{1}_B \right\|_\infty = \left\| \phi\left(\frac{1}{m-1} \sum_{j \in [m-1]} \mathbf{b}_j\right) + \mathbf{1}_B \right\|_\infty \leq O(n^{-\epsilon/16})$$

The proof is given in Section C.1, which simply adopts a concentration bound argument as the random input data has mean 0 and is bounded. By Lemma 1, with uniform attention the input to the next layer collapses to approximately  $-\mathbf{1}_B$ . In a vanilla residual transformer, this collapse propagates: every CoT position’s residual stream contains the noisy near-constant  $-1$ , drowning out the  $O(n^{-2})$  token-distinguishing signal in subsequent layers’ gradients with  $\Omega(n^{-1})$  noise from contractions that should cancel by parity but instead accumulate.

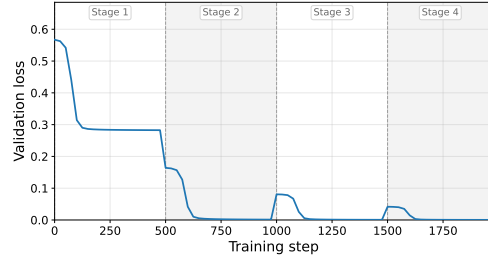
To resolve this, we incorporate gated connections [Srivastava et al., 2015, Parisotto et al., 2020] to replace the residual connections. In the original formulation, the gating weights are input-dependent. In our setting, we instead *prescribe* them from the parity tree’s recursive structure. Specifically, for any  $\ell \in [L]$ , we set the gating weights as:

$$g_m^{(\ell)} = \begin{cases} 1, & n_\ell + 1 \leq m \leq n_{\ell+1}, \\ 0, & \text{otherwise.} \end{cases} \quad (2)$$

Intuitively, layer  $\ell$ ’s gating activates only at level- $(\ell + 1)$  positions  $m \in [n_\ell + 1, n_{\ell+1}]$ , where the layer is responsible for producing the corresponding CoT predictions. At all other positions, the gating mutes the block update, leaving the residual stream to propagate prior content via the block-shift in  $\mathbf{W}_O^{(\ell)}$ . As a consequence, training at each stage focuses gradient signal on a single level of the parity tree, avoiding representation collapse from uniform attention (Lemma 1) at lower-level positions where the loss should not yet be computed. Fixing the gates rather than learning them is what makes the per-stage training dynamics tractable. Each layer’s gradient signal is structurally isolated to its assigned parity-tree level, enabling the layer-wise convergence analysis in Theorem 1.



(a) Customized attention mask.



(b) Validation loss under the Log-ICoT curriculum.

Figure 2: **Attention mask and training dynamics.** Left: illustration of the customized attention mask, where each intermediate state  $\mathbf{x}_m$  at CoT positions ( $m > n$ ) only depends on tokens  $\mathbf{x}_j$  up to the previous level, i.e.,  $j \leq n_{h[m]-1}$ . Right: validation loss of a 4-layer transformer trained under the Log-ICoT curriculum on the  $k$ -parity task ( $n = 30, k = 16$ ); dashed vertical lines mark the four training stages.

**Error propagation.** As we adopt a multi-stage training curriculum, small approximation errors in earlier-stage predictions can compound through the residual stream and overwhelm the gradient signals. To address this, we introduce two modifications to the vanilla transformer model, following Kim and Suzuki [2024].

First, we revise the causal attention mask as in Definition 1 so that each intermediate state  $\mathbf{x}_m$  depends only on tokens at strictly lower levels of the parity tree. This isolates the gradient signal at the correct child positions for our analysis (Lemmas 7 and 9). A visualization of the revised mask can be found in Figure 2(a). Second, we quantize the attention weights after every gradient update by rounding each entry of  $\{\mathbf{W}^{(\ell)}\}_{\ell \in [L]}$  to the nearest integer:

$$\mathbf{W}^{(\ell)}(t+1) = q\left(\mathbf{W}^{(\ell)}(t) - \eta \nabla_{\mathbf{W}^{(\ell)}} \mathcal{L}^{(t)}(\boldsymbol{\theta}(t))\right),$$

where  $q: \mathbb{R} \rightarrow \mathbb{Z}$  is the nearest-integer operator. Integer-based quantization methods are widely used in practice to improve training and inference efficiency [Jacob et al., 2018, Wu et al., 2020], and have also been used in theory to control error propagation in autoregressive generation [Kim and Suzuki, 2024]. In our multi-stage setting, quantization plays an additional role: it locks the weights of previously trained layers. Once a layer is trained, the gradients with respect to its weights at subsequent stages are exponentially small (Lemma 10), so quantization rounds each update back to the trained value. This allows us to analyze stage  $t$  in isolation by treating layers  $1, \dots, t-1$  as fixed.

### 3.3 Main Theorem

We work in the regime  $k = \Theta(n)$ , so  $L = \log_2 k = \Theta(\log n)$  and  $T = n + k - 1 = \Theta(n)$ . The bounded-gradient guarantee  $\|\nabla_{\boldsymbol{\theta}} f_{\boldsymbol{\theta}}^{(t)}(\mathbf{b})\| = O(n^g)$  (Lemma 4) verifies the assumptions of Proposition 1. Without intermediate supervision, no iterative algorithm using  $\text{poly}(n)$  samples and queries can achieve non-trivial accuracy on  $k$ -parity. The following theorem shows that Log-ICoT circumvents this barrier.

**Theorem 1 (Log-ICoT).** *Consider an  $L = \log_2 k$ -layer transformer. Suppose the per-stage batch size satisfies  $B = \Omega(n^{2+\epsilon})$  for some constant  $\epsilon > 0$ , the gradient oracle is  $O(n^{-2-\epsilon/8})$ -accurate, and at each stage  $t \in [L]$ , the learning rate is set to  $\eta_t = \frac{K_n n_t^2}{2c}$ , where  $K_n := \lceil n^{\epsilon/16} \rceil$  and  $c > 0$  is the link function constant in Definition 2. Then for sufficiently large  $n$ , with probability  $1 - \exp(-\Omega(n^{\epsilon/2}))$*

over the random sampling of the training data, the output  $\hat{\boldsymbol{\theta}} = \boldsymbol{\theta}(L)$  of Algorithm 1 satisfies

$$\|f_{\hat{\boldsymbol{\theta}}}^L(\mathbf{D}_{\text{test}})_T - \mathbf{y}_{\text{test}}\|_{\infty} \leq \exp(-\Omega(n^{\epsilon/16})).$$

### 3.4 Proof Sketch

The proof proceeds by induction on the training stage  $t = 1, \dots, L$ , showing that after stage  $t$ , layers  $1, \dots, t$  are *well-trained*, i.e., their attention weights concentrate on the correct two children of each parity node, and the corresponding hidden states approximate the ground-truth parities up to additive error  $\exp(-Cn^{\epsilon/16})$ . We outline the five ingredients below. Figure 4 (Right) in Section B illustrates the residual-stream evolution on a worked example with  $n = 8, k = 4$ .

**Concentration of cross-correlations.** We begin with a probabilistic ingredient that underpins the entire analysis. The choice  $B = \Omega(n^{2+\epsilon})$  is dictated by a Hoeffding-type bound (Lemma 5, following Kim and Suzuki [2024]): with high probability, every non-trivial empirical cross-correlation  $\langle \mathbf{b}_{j_1}, \dots, \mathbf{b}_{j_r} \rangle / B$  between parity terms of order  $r \leq 4$  is at most  $\kappa = O(n^{-1-\epsilon/4})$ . This controls the noise in every gradient computation that follows.

**Stage 1 (Lemma 7).** With concentration in hand, we turn to the base case. All weights are initialized to zero, so layer 1’s attention is uniform. A direct expansion of  $\partial \mathcal{L}^{(1)} / \partial w_{j,m}^{(1)}$  for  $m \in [n+1, n_2]$  using the link function’s Taylor series isolates a signal term of order  $n^{-2}$  at the two children indices  $c_1[m], c_2[m]$ , with all other contributions bounded by  $O(n^{-2-\epsilon/8})$  via the concentration above. With learning rate  $\eta_1 = \Theta(K_n n^2)$ , one gradient step followed by integer quantization yields  $w_{c_1[m],m}^{(1)} = w_{c_2[m],m}^{(1)} = K_n$  and zero elsewhere, producing softmax weights concentrated near 1/2 on the two correct children. The link function then maps the resulting average to the correct parity at every level-2 position, with error  $\exp(-Cn^{\epsilon/16})$ .

**Stage  $t+1$  (Lemma 9).** The inductive step extends this argument upward. Assume the well-trained state holds at stages  $1, \dots, t$ . The same gradient expansion goes through at layer  $t+1$ , but now operating on the *hidden states*  $\mathbf{x}_{j,[t+1]}^{(t)}$  produced by the previous layers rather than raw inputs. Lemma 8 characterizes these hidden states: by the gated connection design (Eq. (2)),  $\mathbf{x}_{j,[t+1]}^{(t)}$  equals  $\mathbf{b}_j$  uniformly up to exponentially small error, so the concentration argument carries over with controlled propagated error.

**Layer freezing across stages.** For the induction to compose, we further need the earlier stages to remain undisturbed. A key feature of Log-ICoT is that once a layer has been trained, it stays trained: at well-trained positions,  $\phi'(\hat{\mathbf{z}}) = O(\exp(-Cn^{\epsilon/16}))$  because  $\hat{\mathbf{z}}$  is exponentially close to a point where  $\phi'$  vanishes (Definition 2). This makes the gradient at every previously trained weight exponentially small, so the quantization operator  $q(\cdot)$  rounds each update back to zero, leaving the weight unchanged. This argument is formalized in Lemma 10. Consequently, we can analyze each layer in isolation, treating earlier layers as fixed.

**Bounding the prediction error.** With the induction in place, it remains to control the propagated error at inference. Let  $\epsilon_t = \max_m \|\mathbf{x}_{m,[t+1]}^{(t)} - \mathbf{b}_m\|_{\infty}$  denote the worst-case approximation error at stage  $t$ . The forward pass induces the recursion

$$\epsilon_{t+1} \leq C_2 (2 \exp(-Cn^{\epsilon/16}) + \epsilon_t)^2,$$

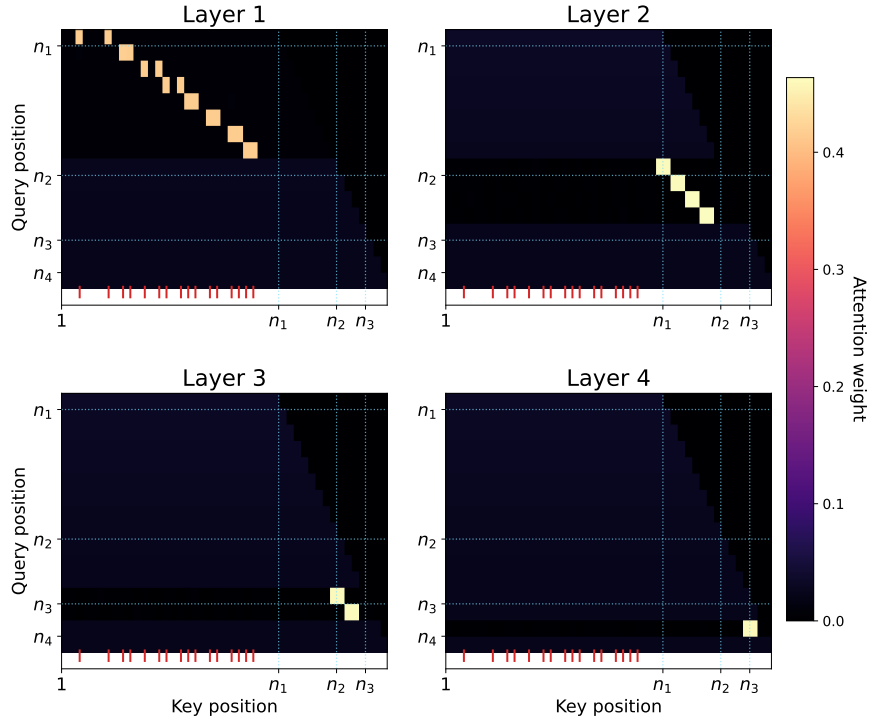


Figure 3: **Layer-wise attention maps of the trained 4-layer transformer at the final stage.** Each panel shows the softmax attention weights at one layer, with rows indexing query positions and columns indexing key positions. Dotted gridlines mark the parity-tree level boundaries  $n_1, n_2, n_3$ . Red ticks on the  $x$ -axis mark the indices in the secret set  $S \subset [n]$ . Each layer’s attention concentrates sharply on the two children of every parity node at its assigned level.

which preserves  $\epsilon_t \leq \exp(-Cn^{\epsilon/16})$  across all  $L = \log_2 k$  stages. At the final stage  $t = L$ , the readout at position  $m = T$  recovers  $\mathbf{y}_{\text{test}}$  up to error  $\exp(-Cn^{\epsilon/16})$ , giving the claimed test error.

## 4 Experiments

We empirically verify the results of Theorem 1 on the  $k$ -parity task, confirming that a multi-layer transformer trained under Log-ICoT converges to the correct parity computation and visualizing how reasoning is progressively internalized into deeper layers. We train a 4-layer simplified transformer (Definition 3) on the  $k$ -parity task with  $n = 30$  and  $k = 16$ , giving  $L = \log_2 k = 4$  training stages. Full details are in Section B.

**Training dynamics.** Figure 2(b) shows the validation loss across the four stages of Log-ICoT. The first stage trains with full reasoning traces visible, after which the loss is already small. At each subsequent stage transition, half of the remaining CoT positions become padded, causing a transient loss spike as the model internalizes one additional parity-tree level into hidden states. The loss then rapidly returns to near zero, consistent with Lemma 7 and Lemma 9. By the end of stage 4, all CoT positions are padded and the model produces the correct parity from input bits alone, reaching 100% validation accuracy.

**Layer-wise internalization.** Figure 3 visualizes the per-layer attention maps at the final stage. Each layer’s attention concentrates sharply on exactly two key positions per query: the two children

of the queried parity node in the tree decomposition. This matches Lemma 9(a), which predicts that softmax weights at each well-trained layer concentrate on the two children of every parity node.

## 5 Conclusion

In this paper, we provide a rigorous theoretical foundation for Implicit Chain-of-Thought (ICoT), demonstrating that multi-layer transformers can internalize complex reasoning processes within their hidden states without sacrificing the sample efficiency gains of explicit CoT. By analyzing the parity learning task, we prove that a multi-layer transformer can achieve polynomial sample complexity while significantly reducing inference latency. Compared to standard ICoT, which removes thinking tokens one at a time, Log-ICoT removes them in geometric chunks, reducing the number of training stages from linear in  $k$  to  $\log_2 k$ . We discuss our limitations and future directions in Section A.

## Acknowledgements

This work was partially supported by a gift from Open Philanthropy to the Center for Human-Compatible AI (CHAI) at UC Berkeley and by NSF Grants IIS-1901252 and CCF-2211209. This work was also supported by NSF grants DMS-2210827, CCF-2315725, CAREER DMS-2339904, ONR grant N00014-24-S-B001, DARPA AIQ grant HR001124S0029-AIQ-FP-003, an Amazon Research Award, a Google Research Scholar Award, an Okawa Foundation Research Grant, and a Sloan Research Fellowship. Y.H. and S.S. were supported by the U.S. Army Research Laboratory and the U.S. Army Research Office under Grant W911NF2010219, Office of Naval Research, and NSF. This work used Jetstream2 at Indiana University through allocation CIS240832 from the Advanced Cyberinfrastructure Coordination Ecosystem: Services & Support (ACCESS) program, which is supported by National Science Foundation grants #2138259, #2138286, #2138307, #2137603, and #2138296.

## References

- Alberto Bietti, Vivien Cabannes, Diane Bouchacourt, Herve Jegou, and Leon Bottou. Birth of a transformer: A memory viewpoint. *Advances in Neural Information Processing Systems*, 36: 1560–1588, 2023.
- Enric Boix-Adsera, Etai Littwin, Emmanuel Abbe, Samy Bengio, and Joshua Susskind. Transformers learn through gradual rank increase. *Advances in Neural Information Processing Systems*, 36: 24519–24551, 2023.
- Lei Chen, Joan Bruna, and Alberto Bietti. Distributional associations vs in-context reasoning: A study of feed-forward and attention layers. *arXiv preprint arXiv:2406.03068*, 2024.
- Yuntian Deng, Kiran Prasad, Roland Fernandez, Paul Smolensky, Vishrav Chaudhary, and Stuart Shieber. Implicit chain of thought reasoning via knowledge distillation. *arXiv preprint arXiv:2311.01460*, 2023.
- Yuntian Deng, Yejin Choi, and Stuart Shieber. From explicit cot to implicit cot: Learning to internalize cot step by step. *arXiv preprint arXiv:2405.14838*, 2024.
- Nelson Elhage, Neel Nanda, Catherine Olsson, Tom Henighan, Nicholas Joseph, Ben Mann, Amanda Askell, Yuntao Bai, Anna Chen, Tom Conerly, Nova DasSarma, Dawn Drain, Deep Ganguli,

- Zac Hatfield-Dodds, Danny Hernandez, Andy Jones, Jackson Kernion, Liane Lovitt, Kamal Ndousse, Dario Amodei, Tom Brown, Jack Clark, Jared Kaplan, Sam McCandlish, and Chris Olah. A mathematical framework for transformer circuits. *Transformer Circuits Thread*, 2021. <https://transformer-circuits.pub/2021/framework/index.html>.
- Guhao Feng, Bohang Zhang, Yuntian Gu, Haotian Ye, Di He, and Liwei Wang. Towards revealing the mystery behind chain of thought: a theoretical perspective. *Advances in Neural Information Processing Systems*, 36:70757–70798, 2023.
- Hengyu Fu, Tianyu Guo, Yu Bai, and Song Mei. What can a single attention layer learn? a study through the random features lens. *Advances in Neural Information Processing Systems*, 36: 11912–11951, 2023.
- Sachin Goyal, Ziwei Ji, Ankit Singh Rawat, Aditya Krishna Menon, Sanjiv Kumar, and Vaishnavh Nagarajan. Think before you speak: Training language models with pause tokens. *arXiv preprint arXiv:2310.02226*, 2023.
- Halil Alperen Gozeten, M Emrullah Ildiz, Xuechen Zhang, Hrayr Harutyunyan, Ankit Singh Rawat, and Samet Oymak. Continuous chain of thought enables parallel exploration and reasoning. *arXiv preprint arXiv:2505.23648*, 2025.
- Tianyu Guo, Druv Pai, Yu Bai, Jiantao Jiao, Michael I Jordan, and Song Mei. Active-dormant attention heads: Mechanistically demystifying extreme-token phenomena in llms. *arXiv preprint arXiv:2410.13835*, 2024.
- Tianyu Guo, Hanlin Zhu, Ruiqi Zhang, Jiantao Jiao, Song Mei, Michael I Jordan, and Stuart Russell. How do llms perform two-hop reasoning in context? *arXiv preprint arXiv:2502.13913*, 2025.
- Shibo Hao, Sainbayar Sukhbaatar, DiJia Su, Xian Li, Zhiting Hu, Jason Weston, and Yuandong Tian. Training large language models to reason in a continuous latent space. *arXiv preprint arXiv:2412.06769*, 2024.
- Jianhao Huang, Zixuan Wang, and Jason D Lee. Transformers learn to implement multi-step gradient descent with chain of thought. *arXiv preprint arXiv:2502.21212*, 2025a.
- Yixiao Huang, Hanlin Zhu, Tianyu Guo, Jiantao Jiao, Somayeh Sojoudi, Michael I Jordan, Stuart Russell, and Song Mei. Generalization or hallucination? understanding out-of-context reasoning in transformers. *arXiv preprint arXiv:2506.10887*, 2025b.
- Yu Huang, Yuan Cheng, and Yingbin Liang. In-context convergence of transformers. In *Proceedings of the 41st International Conference on Machine Learning*, pages 19660–19722, 2024.
- Jonas Hübötter, Frederike Lübeck, Lejs Behric, Anton Baumann, Marco Bagatella, Daniel Marta, Ido Hakimi, Idan Shenfeld, Thomas Kleine Buening, Carlos Guestrin, et al. Reinforcement learning via self-distillation. *arXiv preprint arXiv:2601.20802*, 2026.
- M Emrullah Ildiz, Yixiao Huang, Yingcong Li, Ankit Singh Rawat, and Samet Oymak. From self-attention to markov models: Unveiling the dynamics of generative transformers. *arXiv preprint arXiv:2402.13512*, 2024.
- Benoit Jacob, Skirmantas Kligys, Bo Chen, Menglong Zhu, Matthew Tang, Andrew Howard, Hartwig Adam, and Dmitry Kalenichenko. Quantization and training of neural networks for efficient

- integer-arithmetic-only inference. In *Proceedings of the IEEE conference on computer vision and pattern recognition*, pages 2704–2713, 2018.
- Samy Jelassi, Michael Sander, and Yuanzhi Li. Vision transformers provably learn spatial structure. *Advances in Neural Information Processing Systems*, 35:37822–37836, 2022.
- Tushar Khot, Harsh Trivedi, Matthew Finlayson, Yao Fu, Kyle Richardson, Peter Clark, and Ashish Sabharwal. Decomposed prompting: A modular approach for solving complex tasks. *arXiv preprint arXiv:2210.02406*, 2022.
- Juno Kim and Taiji Suzuki. Transformers provably solve parity efficiently with chain of thought. *arXiv preprint arXiv:2410.08633*, 2024.
- Juncai Li, Ru Li, Yuxiang Zhou, and Jeff Z. Pan. Dissecting implicit chain of thought: Can transformers learn it spontaneously?, 2026. URL <https://openreview.net/forum?id=loP9q6E5kQ>.
- Yingcong Li, Yixiao Huang, Muhammed E Ildiz, Ankit Singh Rawat, and Samet Oymak. Mechanics of next token prediction with self-attention. In *International Conference on Artificial Intelligence and Statistics*, pages 685–693. PMLR, 2024a.
- Zhiyuan Li, Hong Liu, Denny Zhou, and Tengyu Ma. Chain of thought empowers transformers to solve inherently serial problems. *arXiv preprint arXiv:2402.12875*, 1, 2024b.
- Bingbin Liu, Jordan T Ash, Surbhi Goel, Akshay Krishnamurthy, and Cyril Zhang. Transformers learn shortcuts to automata. *arXiv preprint arXiv:2210.10749*, 2022.
- Charles London and Varun Kanade. Pause tokens strictly increase the expressivity of constant-depth transformers. *arXiv preprint arXiv:2505.21024*, 2025.
- Xutao Ma, Yixiao Huang, Hanlin Zhu, and Somayeh Sojoudi. Breaking the reversal curse in autoregressive language models via identity bridge. *arXiv preprint arXiv:2602.02470*, 2026.
- Arvind Mahankali, Tatsunori B Hashimoto, and Tengyu Ma. One step of gradient descent is provably the optimal in-context learner with one layer of linear self-attention. *arXiv preprint arXiv:2307.03576*, 2023.
- Will Merrill and Ashish Sabharwal. Exact expressive power of transformers with padding. *Advances in Neural Information Processing Systems*, 38:112497–112524, 2026.
- William Merrill and Ashish Sabharwal. The expressive power of transformers with chain of thought. *arXiv preprint arXiv:2310.07923*, 2023.
- Eshaan Nichani, Alex Damian, and Jason D Lee. How transformers learn causal structure with gradient descent. In *International Conference on Machine Learning*, pages 38018–38070. PMLR, 2024.
- Emilio Parisotto, Francis Song, Jack Rae, Razvan Pascanu, Caglar Gulcehre, Siddhant Jayakumar, Max Jaderberg, Raphael Lopez Kaufman, Aidan Clark, Seb Noury, et al. Stabilizing transformers for reinforcement learning. In *International conference on machine learning*, pages 7487–7498. PMLR, 2020.
- Jacob Pfau, William Merrill, and Samuel R Bowman. Let’s think dot by dot: Hidden computation in transformer language models. *arXiv preprint arXiv:2404.15758*, 2024.

- Yunwei Ren, Zixuan Wang, and Jason D Lee. Learning and transferring sparse contextual bigrams with linear transformers. In *The Thirty-eighth Annual Conference on Neural Information Processing Systems*, 2024.
- Shai Shalev-Shwartz, Ohad Shamir, and Shaked Shammah. Failures of gradient-based deep learning. In *International Conference on Machine Learning*, pages 3067–3075. PMLR, 2017.
- Zhihong Shao, Peiyi Wang, Qihao Zhu, Runxin Xu, Junxiao Song, Xiao Bi, Haowei Zhang, Mingchuan Zhang, YK Li, Y Wu, et al. Deepseekmath: Pushing the limits of mathematical reasoning in open language models. *arXiv preprint arXiv:2402.03300*, 2024.
- Rupesh Kumar Srivastava, Klaus Greff, and Jürgen Schmidhuber. Highway networks. *arXiv preprint arXiv:1505.00387*, 2015.
- DiJia Su, Hanlin Zhu, Yingchen Xu, Jiantao Jiao, Yuandong Tian, and Qinqing Zheng. Token assorted: Mixing latent and text tokens for improved language model reasoning. *arXiv preprint arXiv:2502.03275*, 2025.
- Yuandong Tian, Yiping Wang, Beidi Chen, and Simon S Du. Scan and snap: Understanding training dynamics and token composition in 1-layer transformer. *Advances in neural information processing systems*, 36:71911–71947, 2023a.
- Yuandong Tian, Yiping Wang, Zhenyu Zhang, Beidi Chen, and Simon Du. Joma: Demystifying multilayer transformers via joint dynamics of mlp and attention. *arXiv preprint arXiv:2310.00535*, 2023b.
- Peiyi Wang, Lei Li, Zhihong Shao, RX Xu, Damai Dai, Yifei Li, Deli Chen, Yu Wu, and Zhifang Sui. Math-shepherd: Verify and reinforce llms step-by-step without human annotations. *arXiv preprint arXiv:2312.08935*, 2023a.
- Xinyi Wang, Lucas Caccia, Oleksiy Ostapenko, Xingdi Yuan, William Yang Wang, and Alessandro Sordani. Guiding language model reasoning with planning tokens. *arXiv preprint arXiv:2310.05707*, 2023b.
- Zixuan Wang, Stanley Wei, Daniel Hsu, and Jason D. Lee. Transformers provably learn sparse token selection while fully-connected nets cannot. In *ICML*, 2024.
- Zixuan Wang, Eshaan Nichani, Alberto Bietti, Alex Damian, Daniel Hsu, Jason D Lee, and Denny Wu. Learning compositional functions with transformers from easy-to-hard data. *arXiv preprint arXiv:2505.23683*, 2025.
- Jason Wei, Xuezhi Wang, Dale Schuurmans, Maarten Bosma, Fei Xia, Ed Chi, Quoc V Le, Denny Zhou, et al. Chain-of-thought prompting elicits reasoning in large language models. *Advances in neural information processing systems*, 35:24824–24837, 2022.
- Kaiyue Wen, Huaqing Zhang, Hongzhou Lin, and Jingzhao Zhang. From sparse dependence to sparse attention: unveiling how chain-of-thought enhances transformer sample efficiency. *arXiv preprint arXiv:2410.05459*, 2024.
- Noam Wies, Yoav Levine, and Amnon Shashua. Sub-task decomposition enables learning in sequence to sequence tasks. *arXiv preprint arXiv:2204.02892*, 2022.

- Hao Wu, Patrick Judd, Xiaojie Zhang, Mikhail Isaev, and Paulius Micikevicius. Integer quantization for deep learning inference: Principles and empirical evaluation. *arXiv preprint arXiv:2004.09602*, 2020.
- Shufang Xie, Huishuai Zhang, Junliang Guo, Xu Tan, Jiang Bian, Hany Hassan Awadalla, Arul Menezes, Tao Qin, and Rui Yan. Residual: Transformer with dual residual connections. *arXiv preprint arXiv:2304.14802*, 2023.
- Longhui Yu, Weisen Jiang, Han Shi, Jincheng Yu, Zhengying Liu, Yu Zhang, James T Kwok, Zhenguo Li, Adrian Weller, and Weiyang Liu. Metamath: Bootstrap your own mathematical questions for large language models. *arXiv preprint arXiv:2309.12284*, 2023.
- Xiang Yue, Xingwei Qu, Ge Zhang, Yao Fu, Wenhao Huang, Huan Sun, Yu Su, and Wenhui Chen. Mammoth: Building math generalist models through hybrid instruction tuning. *arXiv preprint arXiv:2309.05653*, 2023.
- Ruiqi Zhang, Spencer Frei, and Peter L Bartlett. Trained transformers learn linear models in-context. *Journal of Machine Learning Research*, 25(49):1–55, 2024.
- Siyao Zhao, Zhihui Xie, Mengchen Liu, Jing Huang, Guan Pang, Feiyu Chen, and Aditya Grover. Self-distilled reasoner: On-policy self-distillation for large language models. *arXiv preprint arXiv:2601.18734*, 2026.
- Denny Zhou, Nathanael Schärli, Le Hou, Jason Wei, Nathan Scales, Xuezhi Wang, Dale Schuurmans, Claire Cui, Olivier Bousquet, Quoc Le, et al. Least-to-most prompting enables complex reasoning in large language models. *arXiv preprint arXiv:2205.10625*, 2022.
- Defa Zhu, Hongzhi Huang, Zihao Huang, Yutao Zeng, Yunyao Mao, Banggu Wu, Qiyang Min, and Xun Zhou. Hyper-connections. *arXiv preprint arXiv:2409.19606*, 2024a.
- Hanlin Zhu, Baihe Huang, Shaolun Zhang, Michael Jordan, Jiantao Jiao, Yuandong Tian, and Stuart J Russell. Towards a theoretical understanding of the ‘reversal curse’ via training dynamics. *Advances in Neural Information Processing Systems*, 37:90473–90513, 2024b.
- Hanlin Zhu, Shibo Hao, Zhiting Hu, Jiantao Jiao, Stuart Russell, and Yuandong Tian. Emergence of superposition: Unveiling the training dynamics of chain of continuous thought. *arXiv preprint arXiv:2509.23365*, 2025a.
- Hanlin Zhu, Shibo Hao, Zhiting Hu, Jiantao Jiao, Stuart Russell, and Yuandong Tian. Reasoning by superposition: A theoretical perspective on chain of continuous thought. *arXiv preprint arXiv:2505.12514*, 2025b.

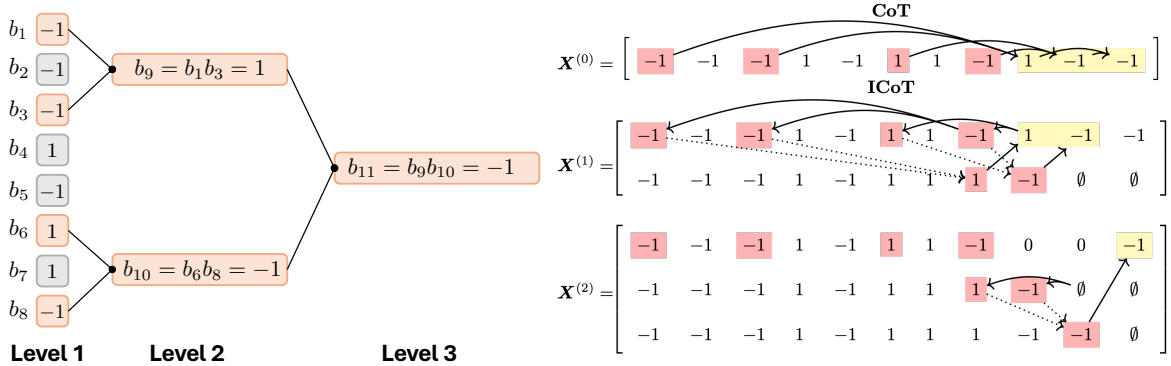


Figure 4: **Illustration of parity learning task with input length  $n = 8$  and secret set size  $k = 4$ .** *Left:* The task can be decomposed into a hierarchical two-parity computation. *Right:* Comparison of the training curriculum of Chain-of-Thought (CoT) and Implicit CoT (ICoT). Both methods initially leverage complete thinking traces derived from the hierarchical decomposition. As the ICoT curriculum progresses, these intermediate reasoning steps are replaced by padding tokens (0), forcing the model to internalize the computation within its hidden states.

## A Limitations and Future Directions

Our analysis relies on several simplifications. To make the multi-layer training dynamics tractable, we train only the attention matrix while fixing the other components: identity value matrices, a link function in place of MLPs, and prescribed output matrices and gating weights. Making the gates input-dependent or trainable, as in Parisotto et al. [2020], Zhu et al. [2024a], is a natural next step. Our experiments are also limited to the synthetic parity task and a four-layer transformer. Although Deng et al. [2024] demonstrate the effectiveness of ICoT on practical reasoning tasks, implementing Log-ICoT in LLMs would require a heuristic for dividing the curriculum into stages, which is non-trivial without the explicit hierarchical structure that parity provides. Finally, we view connecting ICoT to self-distillation [Zhao et al., 2026, Hübötter et al., 2026] as a promising direction. Empirical work [Hübötter et al., 2026] in that line observes that reasoning traces shorten substantially after training, suggesting that a similar internalization mechanism may be at play.

## B Additional Details

### B.1 Example of the Parity-Learning Decomposition

To complement the abstract definitions in Section 2.1 and the proof sketch in Section 3.4, Figure 4 provides a concrete worked example with  $n = 8$  input bits and secret set size  $k = 4$ . The left panel illustrates the hierarchical decomposition of the  $k$ -parity task into a binary tree of two-parity computations: each internal node  $b_m$  ( $m > n$ ) computes the parity of its two children, with the root  $b_{11}$  recovering the target label  $y$ . The right panel illustrates the residual-stream evolution  $\mathbf{X}^{(0)}$ ,  $\mathbf{X}^{(1)}$ ,  $\mathbf{X}^{(2)}$  across layers, contrasting explicit CoT (top) with the ICoT curriculum (bottom), where intermediate reasoning positions are progressively replaced by padding tokens (0) and the model must internalize the computation in its hidden states.

## B.2 Implementation Details

We provide additional implementation details of Section 4.

**Link function.** Following Definition 2, we require a smooth  $\phi$  satisfying  $\phi(0) = -1$ ,  $\phi(\pm 1) = 1$ , and  $\phi'(0) = \phi'(\pm 1) = 0$ . We use the cosine link  $\phi(t) = -\cos(\pi t)$ , which satisfies all three conditions exactly:  $\phi'(t) = \pi \sin(\pi t)$  vanishes at  $t \in \{0, \pm 1\}$ . Its local Taylor expansion around the origin,  $\phi(t) = -1 + \frac{\pi^2}{2}t^2 + O(t^4)$ , matches the form  $\phi(t) = -1 + ct^2 + O(t^4)$  used in our analysis with constant  $c = \pi^2/2$ .

**Data generation.** Inputs are sampled uniformly from  $\{\pm 1\}^n$  with  $n = 30$ . The secret set  $S \subset [n]$  with  $|S| = k = 16$  is sampled uniformly from all size- $k$  subsets of  $[n]$  at the start of training and held fixed thereafter. The label  $y = \prod_{j \in S} b_j$  is computed deterministically from the input. CoT positions  $b_{n+1}, \dots, b_T$  are computed via the recursion  $b_m = b_{c_1[m]} \cdot b_{c_2[m]}$  on the parity tree.

**Training and evaluation.** We optimize with AdamW at learning rate  $10^{-1}$  and batch size 500, run 500 steps per stage for a total of 2,000 training steps, and evaluate on 2,000 held-out samples every 25 steps.

## C Proof of Section 3

**Notations.** Recall from Section 2.1 that  $b_1, \dots, b_n$  are i.i.d. uniform on  $\{\pm 1\}^n$  and that  $b_{n+1}, \dots, b_T$  are determined by the parity-tree recursion based on the secret set  $S$ . For a tuple of indices  $(j_1, \dots, j_r) \in [T]^r$ , we say a parity product  $b_{j_1} \cdots b_{j_r}$  is *trivial* if it always equals 1. E.g., the parity  $b_1 b_3 b_9$  is trivial in Figure 4. We define the set of non-trivial tuples of length  $r$  over the first  $m$  indices as:

$$I_{r,m} = \{(j_1, \dots, j_r) \in [m]^r, b_{j_1} \cdots b_{j_r} \neq 1\}.$$

For  $r = 1$ , every index is non-trivial so  $I_{1,m} = [m]$ . As defined in Section 2.2,  $\Psi_{t'}^\top \mathbf{W}_O^{(t)} = \mathbb{1}(t = t') [\mathbf{0}_{B \times T}, \mathbf{e}_{L+1,t}^\top \otimes \mathbf{I}_B] \in \mathbb{R}^{B \times d}$ . Let  $\mathbf{S}_t = \mathbf{e}_{L+1,t}^\top \otimes \mathbf{I}_B \in \mathbb{R}^{B \times B_L}$ , we denote  $\mathbf{P}_t = \Psi_t^\top \mathbf{W}_O^{(t)} = [\mathbf{0}_{B \times T}, \mathbf{S}_t]$ , which extracts the  $t$ -th  $B$ -dimensional block. For any  $\mathbf{x} \in \mathbb{R}^d$ , we define the  $t$ -th  $B$ -block (after the first  $T$  coordinates) by

$$\mathbf{x}_{[t]} := \mathbf{S}_t \mathbf{x}_T \in \mathbb{R}^B.$$

Equivalently, we have  $(\mathbf{x}_{[t]})_i = x_{T+B(t-1)+i}$ . Finally, for  $x \in \mathbb{R}$  and  $S \subseteq \mathbb{R}$ , we write  $\text{dist}(x, S) := \inf_{s \in S} |x - s|$ .

### C.1 Proof of Lemma 1

*Proof.* Fix any  $n^{\epsilon/8} \leq m \leq n$ . Since  $\mathbf{b}_\alpha \sim \text{Unif}(\{\pm 1\}^B)$  for  $\alpha \in [m]$ . By Hoeffding's inequality, we have that:

$$Pr\left(\left\|\frac{1}{m-1} \sum_{\alpha \in [m-1]} \mathbf{b}_\alpha\right\|_\infty \geq t\right) \leq 2B \exp\left(-\frac{mt^2}{2}\right).$$

Thus with probability  $1 - p_1$ , we have:

$$\left\|\frac{1}{m-1} \sum_{\alpha \in [m-1]} \mathbf{b}_\alpha\right\|_\infty \leq \sqrt{\frac{2}{m} \log(2B/p_1)}.$$

Since  $\phi$  behaves like a quadratic near  $0, \pm 1$ , there exists some constant  $C_2 > 0$  that depends only on  $\phi$  such that

$$\begin{aligned} \left\| \phi\left(\frac{1}{m-1} \sum_{\alpha \in [m-1]} \mathbf{b}_\alpha\right) + \mathbf{1}_B \right\|_\infty &= \left\| \phi\left(\frac{1}{m-1} \sum_{\alpha \in [m-1]} \mathbf{b}_\alpha\right) - \phi(\mathbf{0}_B) \right\|_\infty \leq C_2 \left( \sqrt{\frac{2}{m} \log(2B/p_1)} \right)^2 \\ &\leq C_2 \frac{2}{m} \log(2B/p_1). \end{aligned}$$

Finally, assume the failure probability for each  $m$  be  $\delta_m = p_1/T$ . With probability  $1 - p_1$ , for all  $n^{\epsilon/8} \leq m \leq T < 2n$ , we have

$$\left\| \phi\left(\frac{1}{m-1} \sum_{\alpha \in [m-1]} \mathbf{b}_\alpha\right) + \mathbf{1}_B \right\|_\infty \leq C_2 \frac{2}{m} \log(2TB/p_1).$$

Recall  $B = \text{poly}(n)$  and set  $p_1 = \exp(-n^{\epsilon/16})$ , we have

$$\left\| \phi\left(\frac{1}{m-1} \sum_{\alpha \in [m-1]} \mathbf{b}_\alpha\right) + \mathbf{1}_B \right\|_\infty \leq O(n^{-\epsilon/16}).$$

□

## C.2 Residual stream and gradient propagation

**Lemma 2** (Gated Connection Propagation). *Using the gating weights in Eq. (2), for any position  $\beta \in [T]$  with  $\nu := h[\beta]$ . The residual stream satisfies:*

$$\mathbf{x}_{\beta, [\ell+1]}^{(\ell)} = \begin{cases} \mathbf{x}_{\beta, [1]}^{(0)}, & \nu = 1 \text{ or } 0 \leq \ell < \nu - 1, \\ \phi(\hat{\mathbf{z}}_{\beta, [\nu-1]}^{(\nu-1)}), & \nu \geq 2 \text{ and } \ell \geq \nu - 1. \end{cases}$$

*Proof.* Recall the gated connection update at layer  $\ell$ :

$$\mathbf{x}_\beta^{(\ell)} = \mathbf{x}_\beta^{(\ell-1)} + \mathbf{W}_\mathbf{O}^{(\ell)} \cdot \text{GC}_\beta^{(\ell)},$$

where  $\text{GC}_\beta^{(\ell)} = g_\beta^{(\ell)} \phi(\hat{\mathbf{z}}_\beta^{(\ell)}) + (1 - g_\beta^{(\ell)}) \mathbf{x}_\beta^{(\ell-1)}$  and  $\mathbf{W}_\mathbf{O}^{(\ell)}$  is the block-shift operator that places content from residual block  $[\ell]$  to block  $[\ell + 1]$ .

Componentwise, the block- $[\ell + 1]$  update at position  $\beta$  reads

$$\mathbf{x}_{\beta, [\ell+1]}^{(\ell)} = \mathbf{x}_{\beta, [\ell+1]}^{(\ell-1)} + g_\beta^{(\ell)} \phi(\hat{\mathbf{z}}_{\beta, [\ell]}^{(\ell)}) + (1 - g_\beta^{(\ell)}) \mathbf{x}_{\beta, [\ell]}^{(\ell-1)}, \quad (\star)$$

while blocks  $[k]$  for  $k \neq \ell + 1$  are preserved, i.e.,  $\mathbf{x}_{\beta, [k]}^{(\ell)} = \mathbf{x}_{\beta, [k]}^{(\ell-1)}$  for  $k \neq \ell + 1$ .

Recall the per-block gating from Eq. (2):

$$g_\beta^{(\ell)} = \begin{cases} 1, & n_\ell + 1 \leq \beta \leq n_{\ell+1}, \\ 0, & \text{otherwise.} \end{cases}$$

Hence  $g_\beta^{(\ell)} = 1$  iff  $\ell = \nu - 1$  (the writing layer for position  $\beta$ ); otherwise  $g_\beta^{(\ell)} = 0$ .

**Case 1:  $\nu = 1$  (input position).** For  $\beta \leq n$ ,  $g_\beta^{(\ell)} = 0$  for all  $\ell$ , so Eq. (★) reduces to

$$\mathbf{x}_{\beta, [\ell+1]}^{(\ell)} = \mathbf{x}_{\beta, [\ell+1]}^{(\ell-1)} + \mathbf{x}_{\beta, [\ell]}^{(\ell-1)}.$$

We prove by induction on  $\ell$  that  $\mathbf{x}_{\beta, [\ell+1]}^{(\ell)} = \mathbf{x}_{\beta, [1]}^{(0)}$  for all  $\ell \geq 0$ . The base case  $\ell = 0$  holds trivially. For the inductive step, assume  $\mathbf{x}_{\beta, [\ell]}^{(\ell-1)} = \mathbf{x}_{\beta, [1]}^{(0)}$ . Block  $[\ell + 1]$  is unchanged at all earlier layers (since the writing layer for block  $[\ell + 1]$  is layer  $\ell$ , and earlier layers don't touch block  $[\ell + 1]$ ). Hence  $\mathbf{x}_{\beta, [\ell+1]}^{(\ell-1)} = \mathbf{x}_{\beta, [\ell+1]}^{(0)} = \mathbf{0}_B$  (Section 2.2, the embedding has only block [1] nonzero). Therefore

$$\mathbf{x}_{\beta, [\ell+1]}^{(\ell)} = \mathbf{0}_B + \mathbf{x}_{\beta, [1]}^{(0)} = \mathbf{x}_{\beta, [1]}^{(0)}.$$

**Case 2:  $\nu \geq 2$  and  $0 \leq \ell < \nu - 1$  (before writing layer).** For these layers,  $g_\beta^{(\ell)} = 0$ , so Eq. (★) again reduces to

$$\mathbf{x}_{\beta, [\ell+1]}^{(\ell)} = \mathbf{x}_{\beta, [\ell+1]}^{(\ell-1)} + \mathbf{x}_{\beta, [\ell]}^{(\ell-1)}.$$

By the same induction on  $\ell$  as in Case 1,  $\mathbf{x}_{\beta, [\ell+1]}^{(\ell)} = \mathbf{x}_{\beta, [1]}^{(0)}$  for  $0 \leq \ell < \nu - 1$ . Note that  $\mathbf{x}_{\beta, [1]}^{(0)}$  here is the embedding content at position  $\beta$ , which can be  $\mathbf{b}_\beta$  (shown CoT) or  $\mathbf{0}_B$  (padded CoT) depending on the curriculum's stage.

**Case 3:  $\nu \geq 2$  and  $\ell = \nu - 1$  (writing layer).** At the writing layer,  $g_\beta^{(\nu-1)} = 1$ , so Eq. (★) becomes

$$\mathbf{x}_{\beta, [\nu]}^{(\nu-1)} = \mathbf{x}_{\beta, [\nu]}^{(\nu-2)} + \phi(\hat{\mathbf{z}}_{\beta, [\nu-1]}^{(\nu-1)}).$$

Block  $[\nu]$  has not been written by any earlier layer (the writing layer for block  $[\nu]$  is layer  $\nu - 1$ , the current layer). Hence  $\mathbf{x}_{\beta, [\nu]}^{(\nu-2)} = \mathbf{x}_{\beta, [\nu]}^{(0)} = \mathbf{0}_B$ . Therefore

$$\mathbf{x}_{\beta, [\nu]}^{(\nu-1)} = \phi(\hat{\mathbf{z}}_{\beta, [\nu-1]}^{(\nu-1)}).$$

**Case 4:  $\nu \geq 2$  and  $\ell \geq \nu$  (after writing layer).** For  $\ell \geq \nu$ ,  $g_\beta^{(\ell)} = 0$  (since  $\beta \leq n_{\ell-1} < n_\ell + 1$ ), so Eq. (★) reduces to

$$\mathbf{x}_{\beta, [\ell+1]}^{(\ell)} = \mathbf{x}_{\beta, [\ell+1]}^{(\ell-1)} + \mathbf{x}_{\beta, [\ell]}^{(\ell-1)}.$$

We prove by induction on  $\ell \geq \nu$  that  $\mathbf{x}_{\beta, [\ell+1]}^{(\ell)} = \phi(\hat{\mathbf{z}}_{\beta, [\nu-1]}^{(\nu-1)})$ . The base case  $\ell = \nu - 1$  is Case 3.

For  $\ell \geq \nu$ : by the inductive hypothesis applied at  $\ell - 1 \geq \nu - 1$ ,  $\mathbf{x}_{\beta, [\ell]}^{(\ell-1)} = \phi(\hat{\mathbf{z}}_{\beta, [\nu-1]}^{(\nu-1)})$ . Block  $[\ell + 1]$  has not been written at any earlier layer, so  $\mathbf{x}_{\beta, [\ell+1]}^{(\ell-1)} = \mathbf{0}_B$ . Therefore

$$\mathbf{x}_{\beta, [\ell+1]}^{(\ell)} = \mathbf{0}_B + \phi(\hat{\mathbf{z}}_{\beta, [\nu-1]}^{(\nu-1)}) = \phi(\hat{\mathbf{z}}_{\beta, [\nu-1]}^{(\nu-1)}).$$

Combining Cases 1, 2 (which give  $\mathbf{x}_{\beta, [1]}^{(0)}$ ) and Cases 3, 4 (which give  $\phi(\hat{\mathbf{z}}_{\beta, [\nu-1]}^{(\nu-1)})$ ), the lemma follows.  $\square$

**Corollary 1 (Frozen Derivative).** *Under the setting of Lemma 2, for any  $\beta \in [T]$  with  $\nu := h[\beta]$ , any layer  $\ell \in \{0, \dots, L\}$ , and any parameter  $w_{j,m}^{(\ell')}$  with  $\ell' \in [L]$ :*

$$\frac{\partial \mathbf{x}_{\beta, [\ell+1]}^{(\ell)}}{\partial w_{j,m}^{(\ell')}} = \begin{cases} \frac{\partial \phi(\hat{\mathbf{z}}_{\beta, [\nu-1]}^{(\nu-1)})}{\partial w_{j,m}^{(\ell')}}, & \nu \geq 2, \ell \geq \nu - 1, \ell' \leq \nu - 1, \\ \mathbf{0}, & \text{otherwise.} \end{cases}$$

*Proof.* By Lemma 2,  $\mathbf{x}_{\beta, [\ell+1]}^{(\ell)}$  takes two forms:

- If  $\nu = 1$ , or if  $\nu \geq 2$  with  $\ell < \nu - 1$ :  $\mathbf{x}_{\beta, [\ell+1]}^{(\ell)} = \mathbf{x}_{\beta, [1]}^{(0)}$ . The embedding is data, not a trainable parameter, so the derivative vanishes.
- If  $\nu \geq 2$  and  $\ell \geq \nu - 1$ :  $\mathbf{x}_{\beta, [\ell+1]}^{(\ell)} = \phi(\hat{\mathbf{z}}_{\beta, [\nu-1]}^{(\nu-1)})$ . By chain rule,

$$\frac{\partial \mathbf{x}_{\beta, [\ell+1]}^{(\ell)}}{\partial w_{j,m}^{(\ell')}} = \frac{\partial \phi(\hat{\mathbf{z}}_{\beta, [\nu-1]}^{(\nu-1)})}{\partial w_{j,m}^{(\ell')}}.$$

Since  $\phi(\hat{\mathbf{z}}_{\beta, [\nu-1]}^{(\nu-1)})$  depends only on  $\{\mathbf{W}^{(\tau)}\}_{\tau \leq \nu-1}$ , the derivative vanishes when  $\ell' > \nu - 1$ , and equals the chain-rule expression when  $\ell' \leq \nu - 1$ .

In all sub-cases, the derivative matches the corollary's statement.  $\square$

**Lemma 3** (Per-Node Sensitivity). *Let  $L_\phi := \|\phi'\|_\infty$ . For any layer indices  $\ell' \leq \ell \leq L$ , any query position  $m \in [n_{\ell'} + 1, n_{\ell'+1}]$ , and any  $1 \leq j \leq m - 1$ , define*

$$\xi_{j,m,\ell'}^{(\ell)} := \max_{\beta: h[\beta] \leq \ell+1} \left\| \frac{\partial \mathbf{x}_{\beta, [\ell+1]}^{(\ell)}}{\partial w_{j,m}^{(\ell')}} \right\|_\infty.$$

Then

$$\xi_{j,m,\ell'}^{(\ell)} \leq 2L_\phi^{\ell-\ell'+1} \sigma_j(\mathbf{w}_m^{(\ell')}).$$

*Proof.* We induct on  $\ell$ .

**Base case**  $\ell = \ell'$ . By Corollary 1, the derivative is nonzero only when  $\nu \geq 2$ ,  $\ell' \geq \nu - 1$ , and  $\ell' \leq \nu - 1$ , i.e.,  $\nu - 1 = \ell'$ , so  $\nu = \ell' + 1$ . For positions with  $\nu > \ell' + 1$ , the derivative vanishes since the residual equals the embedding which is not a trainable parameter. For positions with  $\nu \leq \ell'$ , the writing layer is at most  $\ell' - 1 < \ell'$ , so the derivative also vanishes by Corollary 1.

Hence only  $\beta$  with  $\nu = \ell' + 1$  contribute. For such  $\beta$ , Corollary 1 yields

$$\frac{\partial \mathbf{x}_{\beta, [\ell'+1]}^{(\ell')}}{\partial w_{j,m}^{(\ell')}} = \frac{\partial \phi(\hat{\mathbf{z}}_{\beta, [\ell']}^{(\ell')})}{\partial w_{j,m}^{(\ell')}} = \phi'(\hat{\mathbf{z}}_{\beta, [\ell']}^{(\ell')}) \odot \frac{\partial \hat{\mathbf{z}}_{\beta, [\ell']}^{(\ell')}}{\partial w_{j,m}^{(\ell')}}.$$

The parameter  $w_{j,m}^{(\ell')}$  enters  $\hat{\mathbf{z}}_{\beta}^{(\ell')}$  only through the softmax weights at query position  $\beta = m$ , giving

$$\frac{\partial \hat{\mathbf{z}}_{m, [\ell']}^{(\ell')}}{\partial w_{j,m}^{(\ell')}} = \sigma_j(\mathbf{w}_m^{(\ell')}) (\mathbf{x}_{j, [\ell']}^{(\ell'-1)} - \hat{\mathbf{z}}_{m, [\ell']}^{(\ell')}).$$

Each component of  $\mathbf{x}_{j, [\ell']}^{(\ell'-1)} - \hat{\mathbf{z}}_{m, [\ell']}^{(\ell')}$  lies in  $[-2, 2]$ , so

$$\xi_{j,m,\ell'}^{(\ell')} \leq L_\phi \cdot 2\sigma_j(\mathbf{w}_m^{(\ell')}) = 2L_\phi \sigma_j(\mathbf{w}_m^{(\ell')}),$$

matching the claim with  $\ell - \ell' + 1 = 1$ .

**Inductive step**  $\ell \Rightarrow \ell + 1$ . Take any  $\beta \in [T]$  with  $\nu := h[\beta]$ . By Corollary 1, the derivative is zero unless  $\nu \geq \ell' + 1$  and  $\ell + 1 \geq \nu - 1$ , i.e.,  $\nu \leq \ell + 2$ . So  $\nu \in \{\ell' + 1, \dots, \ell + 2\}$ .

We split into two sub-cases.

*Sub-case A:*  $\nu \leq \ell + 1$ . By Lemma 2, both  $\mathbf{x}_{\beta, [\ell+2]}^{(\ell+1)}$  and  $\mathbf{x}_{\beta, [\ell+1]}^{(\ell)}$  equal the same value  $\phi(\hat{\mathbf{z}}_{\beta, [\nu-1]}^{(\nu-1)})$ , hence have identical derivatives:

$$\left\| \frac{\partial \mathbf{x}_{\beta, [\ell+2]}^{(\ell+1)}}{\partial w_{j,m}^{(\ell')}} \right\|_{\infty} = \left\| \frac{\partial \mathbf{x}_{\beta, [\ell+1]}^{(\ell)}}{\partial w_{j,m}^{(\ell')}} \right\|_{\infty} \leq \xi_{j,m,\ell'}^{(\ell)}.$$

*Sub-case B:*  $\nu = \ell + 2$ . Then  $\beta$ 's writing layer is  $\ell + 1$ , and Corollary 1 gives

$$\frac{\partial \mathbf{x}_{\beta, [\ell+2]}^{(\ell+1)}}{\partial w_{j,m}^{(\ell')}} = \frac{\partial \phi(\hat{\mathbf{z}}_{\beta, [\ell+1]}^{(\ell+1)})}{\partial w_{j,m}^{(\ell')}} = \phi'(\hat{\mathbf{z}}_{\beta, [\ell+1]}^{(\ell+1)}) \odot \frac{\partial \hat{\mathbf{z}}_{\beta, [\ell+1]}^{(\ell+1)}}{\partial w_{j,m}^{(\ell')}}.$$

Since  $\ell' \leq \ell < \ell + 1$ , the parameter  $w_{j,m}^{(\ell')}$  does not enter the softmax weights  $\sigma(\mathbf{w}_{\beta}^{(\ell+1)})$ , so differentiation passes through:

$$\frac{\partial \hat{\mathbf{z}}_{\beta, [\ell+1]}^{(\ell+1)}}{\partial w_{j,m}^{(\ell')}} = \sum_{\gamma=1}^{\beta-1} \sigma_{\gamma}(\mathbf{w}_{\beta}^{(\ell+1)}) \frac{\partial \mathbf{x}_{\gamma, [\ell+1]}^{(\ell)}}{\partial w_{j,m}^{(\ell')}}.$$

Each summand has  $\infty$ -norm at most  $\xi_{j,m,\ell'}^{(\ell)}$ , and the softmax weights sum to at most 1, so

$$\left\| \frac{\partial \hat{\mathbf{z}}_{\beta, [\ell+1]}^{(\ell+1)}}{\partial w_{j,m}^{(\ell')}} \right\|_{\infty} \leq \xi_{j,m,\ell'}^{(\ell)}.$$

Multiplying by  $\|\phi'\|_{\infty} = L_{\phi}$ :

$$\left\| \frac{\partial \mathbf{x}_{\beta, [\ell+2]}^{(\ell+1)}}{\partial w_{j,m}^{(\ell')}} \right\|_{\infty} \leq L_{\phi} \xi_{j,m,\ell'}^{(\ell)}.$$

*Combining sub-cases.* Taking the max over  $\beta$  and using  $L_{\phi} \geq 1$ ,

$$\xi_{j,m,\ell'}^{(\ell+1)} \leq L_{\phi} \xi_{j,m,\ell'}^{(\ell)} \leq L_{\phi} \cdot 2L_{\phi}^{\ell-\ell'+1} \sigma_j(\mathbf{w}_m^{(\ell')}) = 2L_{\phi}^{(\ell+1)-\ell'+1} \sigma_j(\mathbf{w}_m^{(\ell')}).$$

This closes the induction.  $\square$

### C.3 Bounded Gradient

**Lemma 4** (Bounded Gradient). *For any stage  $t \in [L]$ , any input  $\mathbf{b} \in \{\pm 1\}^n$  and any parameters  $\theta$ ,*

$$\|\nabla_{\theta} f_{\theta}^{(t)}(\mathbf{b})\|_2 \leq O(n^g),$$

where  $f_{\theta}^{(t)}(\mathbf{b}) := \Psi_t^{\top} \mathcal{T}_{\theta}(\mathbf{b}) \in \mathbb{R}^T$  is the stage- $t$  model output,  $g = \log_2 L_{\phi} + 1$  and  $L_{\phi} := \|\phi'\|_{\infty}$ .

*Proof.* Fix a stage  $t \in [L]$ . The stage- $t$  model output reads  $f_{\theta}^{(t)}(\mathbf{b}) = \Psi_t^{\top} \mathcal{T}_{\theta}(\mathbf{b})$ , where  $\Psi_t$  extracts block  $[t+1]$ . By Lemma 2, for any  $\alpha \in [T]$  with  $h[\alpha] \leq t+1$ , the readout coordinate is

$$f_{\theta,\alpha}^{(t)}(\mathbf{b}) := (\Psi_t^{\top} \mathcal{T}_{\theta}(\mathbf{b}))_{\alpha} = \mathbf{x}_{\alpha, [t+1]}^{(t)},$$

and for  $\alpha$  with  $h[\alpha] > t+1$ , the readout reduces to the embedding due to Lemma 2 (which has zero gradient). It therefore suffices to bound  $\|\nabla_{\theta} f_{\theta,\alpha}^{(t)}(\mathbf{b})\|$  at each  $\alpha$  with  $h[\alpha] \leq t+1$ , then sum. Fix such an  $\alpha$ .

**Bounding per-parameter derivatives.** For any trainable parameter  $w_{j,m}^{(\ell')}$  with  $\ell' \in [L]$ ,  $n_{\ell'} + 1 \leq m \leq n_{\ell'+1}$ , and  $1 \leq j \leq m - 1$ , Lemma 3 yields

$$\left| \frac{\partial f_{\theta,\alpha}^{(t)}(\mathbf{b})}{\partial w_{j,m}^{(\ell')}} \right| = \left| \frac{\partial \mathbf{x}_{\alpha,[t+1]}^{(t)}}{\partial w_{j,m}^{(\ell')}} \right| \leq \xi_{j,m,\ell'}^{(t)} \leq 2L_\phi^{t-\ell'+1} \sigma_j(\mathbf{w}_m^{(\ell')}).$$

The bound is non-trivial only for  $\ell' \leq t$ ; for  $\ell' > t$ , the derivative vanishes by Corollary 1 since  $\alpha$ 's writing layer  $h[\alpha] - 1 \leq t < \ell'$ .

**Summing over parameters.** We compute  $\|\nabla_\theta f_{\theta,\alpha}^{(t)}(\mathbf{b})\|^2$  by summing the squared derivatives over all trainable parameters. Square the per-parameter bound:

$$\left| \frac{\partial f_{\theta,\alpha}^{(t)}(\mathbf{b})}{\partial w_{j,m}^{(\ell')}} \right|^2 \leq 4L_\phi^{2(t-\ell'+1)} \sigma_j(\mathbf{w}_m^{(\ell')})^2.$$

*Sum over  $j$ .* Using  $\sum_{j=1}^{m-1} \sigma_j(\mathbf{w}_m^{(\ell')})^2 \leq \sum_{j=1}^{m-1} \sigma_j(\mathbf{w}_m^{(\ell')}) = 1$ ,

$$\sum_{j=1}^{m-1} \left| \frac{\partial f_{\theta,\alpha}^{(t)}(\mathbf{b})}{\partial w_{j,m}^{(\ell')}} \right|^2 \leq 4L_\phi^{2(t-\ell'+1)}.$$

*Sum over  $m$ .* Trainable indices  $m$  at layer  $\ell'$  satisfy  $n_{\ell'} + 1 \leq m \leq n_{\ell'+1}$ , with  $n_{\ell'+1} - n_{\ell'} = k \cdot 2^{-\ell'} = O(n)$ , so

$$\sum_{m,j} \left| \frac{\partial f_{\theta,\alpha}^{(t)}(\mathbf{b})}{\partial w_{j,m}^{(\ell')}} \right|^2 \leq O(n) \cdot L_\phi^{2(t-\ell'+1)}.$$

*Sum over  $\ell' \leq t$ .* Letting  $r := t - \ell' + 1$  range over  $1, 2, \dots, t$ ,

$$\sum_{\ell'=1}^t \sum_{m,j} \left| \frac{\partial f_{\theta,\alpha}^{(t)}(\mathbf{b})}{\partial w_{j,m}^{(\ell')}} \right|^2 \leq \sum_{r=1}^t O(n) \cdot L_\phi^{2r} = O(nL_\phi^{2t}).$$

Since  $t \leq L = \log_2 k$  and  $k = O(n)$ ,

$$O(nL_\phi^{2t}) \leq O(nL_\phi^{2L}) = O(n \cdot k^{2 \log_2 L_\phi}) = O(n^{2 \log_2 L_\phi + 1}).$$

Therefore,

$$\|\nabla_\theta f_{\theta,\alpha}^{(t)}(\mathbf{b})\|^2 \leq O(n^{2 \log_2 L_\phi + 1}),$$

which gives  $\|\nabla_\theta f_{\theta,\alpha}^{(t)}(\mathbf{b})\| \leq O(n^{\log_2 L_\phi + 1/2}) = O(n^{g-1/2})$ .

**Conclusion.** Summing over  $\alpha \in [T]$  with  $T = O(n)$ ,

$$\|\nabla_\theta f_\theta^{(t)}(\mathbf{b})\|^2 = \sum_{\alpha} \|\nabla_\theta f_{\theta,\alpha}^{(t)}(\mathbf{b})\|^2 \leq O(n) \cdot O(n^{2g-1}) = O(n^{2g}),$$

giving  $\|\nabla_\theta f_\theta^{(t)}(\mathbf{b})\| \leq O(n^g)$ , as claimed.  $\square$

## C.4 Preliminary Lemmas

**Lemma 5** (Kim and Suzuki [2024], Lemma 9). Recall that  $I_{r,m}$  is defined as the set of non-trivial tuples of length  $r$  over the first  $m$  indices as:

$$I_{r,m} = \{(j_1, \dots, j_r) \in [m]^r, b_{j_1} \cdots b_{j_r} \neq 1\}.$$

Assume  $\mathbf{b}_1, \dots, \mathbf{b}_m \in \{\pm 1\}^B$  are vectors where each bit is sampled i.i.d. from the uniform distribution. For any  $p > 0$ , with probability at least  $1 - p$ , the following holds for all  $r \leq 4$ :

$$\max_{(j_1, \dots, j_r) \in I_{r,m}} \frac{|\langle \mathbf{b}_{j_1}, \dots, \mathbf{b}_{j_r} \rangle|}{B} \leq \kappa := \sqrt{\frac{2}{B} \log \frac{32n^4}{p}}.$$

In particular, we set  $B = \Omega(n^{2+\epsilon})$  for some constant  $\epsilon > 0$  and  $p = \exp(-n^{\epsilon/2})$  such that  $\kappa = O(n^{-1-\epsilon/4})$ . Lemma 5 bounds the contribution of *non-trivial* tuples (those in  $I_{r,m}$ ), where each inner product  $|\langle \mathbf{b}_{j_1}, \dots, \mathbf{b}_{j_r} \rangle|/B$  is at most  $\kappa$ . The complementary contribution comes from *trivial* tuples (those in  $[m]^r \setminus I_{r,m}$ ), where the inner product equals  $B$  deterministically. Bounding such gradient contractions therefore reduces to counting trivial tuples, which we do next for the case  $r = 4$ .

**Lemma 6** (Trivial 4-tuple count). Let  $\mathbf{b}_1, \dots, \mathbf{b}_n \in \{\pm 1\}^B$  be i.i.d. uniform input bits, and for  $\tau \in [n+1, T]$  let  $\mathbf{b}_\tau := \mathbf{b}_{c_1[\tau]} \odot \mathbf{b}_{c_2[\tau]}$  denote the parity defined by the tree (Section 2.1). For any  $m \in [n+1, T]$ , the number of 4-tuples  $(\alpha, \beta, \gamma, \delta) \in [m-1]^4$  with  $\langle \mathbf{b}_\alpha, \mathbf{b}_\beta, \mathbf{b}_\gamma, \mathbf{b}_\delta \rangle$  trivial (i.e.,  $(\alpha, \beta, \gamma, \delta) \notin I_{4,m}$ ) is at most  $O(n^2)$ .

*Proof.* By the bit-counting argument,  $\langle \mathbf{b}_\alpha, \mathbf{b}_\beta, \mathbf{b}_\gamma, \mathbf{b}_\delta \rangle \equiv B$  happens iff the multiset of input bits in the parity product cancels evenly. Without loss of generality, assume  $h[\alpha] \leq h[\beta] \leq h[\gamma] \leq h[\delta]$ . Under the causal mask,  $\alpha, \beta, \gamma, \delta \in [m-1]$  may take any level, so we enumerate by the level structure.

1. If  $h[\beta] < h[\gamma] < h[\delta]$ , to cancel out  $\mathbf{b}_\delta$ , it must hold that  $\mathbf{b}_\gamma$  is a child of  $\mathbf{b}_\delta$  and  $\mathbf{b}_\alpha, \mathbf{b}_\beta$  are the two children of the other child. This is fully determined by choosing  $\delta$  and which child is  $\gamma$ , giving  $O(n)$  trivial 4-tuples.
2. If  $h[\beta] = h[\gamma] < h[\delta]$ , then  $\mathbf{b}_\beta, \mathbf{b}_\gamma$  must both be children of  $\mathbf{b}_\delta$ , requiring  $h[\gamma] = h[\delta] - 1$ . Then  $\langle \mathbf{b}_\beta, \mathbf{b}_\gamma, \mathbf{b}_\delta \rangle = B$ , and for  $\langle \mathbf{b}_\alpha, \mathbf{b}_\beta, \mathbf{b}_\gamma, \mathbf{b}_\delta \rangle$  to be trivial, we would need  $\langle \mathbf{b}_\alpha \rangle = B$ , which is impossible. No trivial 4-tuples.
3. If  $h[\beta] < h[\gamma] = h[\delta]$ , then  $\gamma = \delta$  (since same-level peers cover disjoint bits, two distinct peers cannot have trivial product). This forces  $\alpha = \beta$  similarly. There are  $O(n^2)$  such trivial 4-tuples.
4. If  $h[\alpha] = h[\beta] = h[\gamma] = h[\delta]$ , then the four same-level nodes must pair up to cancel. There are  $O(n^2)$  such trivial 4-tuples.
5. If  $h[\alpha] < h[\beta] = h[\gamma] = h[\delta]$ , then  $\langle \mathbf{b}_\beta, \mathbf{b}_\gamma, \mathbf{b}_\delta \rangle$  involves at least  $2^{h[\beta]-1}$  distinct input bits, so  $\mathbf{b}_\alpha$  would need to cover all these bits for the 4-tuple to be trivial. But  $\mathbf{b}_\alpha$  is a parity over only  $2^{h[\alpha]-1} < 2^{h[\beta]-1}$  bits. No trivial 4-tuples.

Combining cases 1, 3, and 4, the total count of trivial 4-tuples is  $O(n) + O(n^2) + O(n^2) = O(n^2)$ . Cases 2 and 5 contribute none.  $\square$

We now proceed to the main proof of Theorem 1.

## C.5 Proof of Theorem 1

**Definition 4** (Well-trained layer). *Layer  $\ell \in [L]$  is well-trained if:*

- (softmax concentration) For all  $m \in [n_\ell + 1, n_{\ell+1}]$ ,

$$\frac{1 - \exp(-Cn^{\epsilon/16})}{2} \leq \sigma_{c_1[m]}(\mathbf{w}_m^{(\ell)}), \sigma_{c_2[m]}(\mathbf{w}_m^{(\ell)}) \leq \frac{1}{2};$$

- (forward error) For all  $m \in [n_\ell + 1, n_{\ell+1}]$ ,  $\|\mathbf{x}_{m, [\ell+1]}^{(\ell)} - \mathbf{b}_m\|_\infty \leq \exp(-Cn^{\epsilon/16})$ .

**Lemma 7** (Stage 1). *After one-step gradient descent on the stage-1 loss  $\mathcal{L}^{(1)}$  with  $B$  training samples and stage-wise learning rate  $\eta_1 = \frac{K_n n^2}{2c}$ , where  $B = \Omega(n^{2+\epsilon})$ ,  $K_n := \lceil n^{\epsilon/16} \rceil$  and  $c > 0$  is the link function constant in Definition 2, with probability  $1 - \exp(-n^{\epsilon/2})$  over the sampling of  $\mathbf{b}^1, \dots, \mathbf{b}^B$ , layer 1 is well-trained (Definition 4).*

*Proof.* At stage 1, the curriculum's input has  $\mathbf{x}_{\beta, [1]}^{(0)} = \mathbf{b}_\beta$  for all  $\beta \in [T]$  (full CoT). Recall that

$$\mathcal{L}^{(1)}(\boldsymbol{\theta}) = \frac{1}{2B} \sum_{m=n+1}^T \|\Psi_1^\top \mathbf{W}_O^{(1)} \left( g_m^{(1)} \phi \left( \sum_{j=1}^{n_{h[m]}-1} \sigma_j(\mathbf{w}_m^{(1)}) \mathbf{x}_j^{(0)} \right) + (1 - g_m^{(1)}) \mathbf{x}_m^{(0)} \right) - \mathbf{b}_m\|^2.$$

We split into two cases. **Case 1:**  $m > n_2$ . Layer 1 is inactive ( $g_m^{(1)} = 0$ );  $w_{j,m}^{(1)}$  is structurally decoupled from the loss, giving zero gradient. **Case 2:**  $m \in [n+1, n_2]$ . Layer 1 is active ( $g_m^{(1)} = 1$ ). Thus, we analyze the gradient signal in detail and treat Case 1 first.

**Case 1:**  $m > n_2$ . Under per-block gating,  $g_m^{(1)} = 0$ . The gated connection update at position  $m$  becomes

$$\mathbf{x}_{m, [2]}^{(1)} = \mathbf{x}_{m, [2]}^{(0)} + (1 - g_m^{(1)}) \mathbf{x}_{m, [1]}^{(0)} + g_m^{(1)} \phi(\hat{\mathbf{z}}_m^{(1)}) = \mathbf{x}_{m, [2]}^{(0)} + \mathbf{x}_{m, [1]}^{(0)},$$

which does not depend on  $\hat{\mathbf{z}}_m^{(1)}$  and hence not on  $\mathbf{w}_m^{(1)}$ . Therefore  $w_{j,m}^{(1)}$  is absent from  $\mathcal{L}^{(1)}$ , giving  $\partial \mathcal{L}^{(1)} / \partial w_{j,m}^{(1)} = 0$  identically. After quantization,  $w_{j,m}^{(1)}$  remains zero.

**Case 2:**  $m \in [n+1, n_2]$ . For  $m \in [n+1, n_2]$ , the loss term reduces to

$$\frac{1}{2B} \|\Psi_1^\top \mathbf{W}_O^{(1)} \phi(\hat{\mathbf{z}}_m^{(1)}) - \mathbf{b}_m\|^2,$$

where  $\hat{\mathbf{z}}_m^{(1)} = \sum_{j=1}^n \sigma_j(\mathbf{w}_m^{(1)}) \mathbf{x}_j^{(0)}$ . Standard softmax derivative computations give

$$\frac{\partial \hat{\mathbf{z}}_m^{(1)}}{\partial w_{j,m}^{(1)}} = \sigma_j(\mathbf{w}_m^{(1)}) (\mathbf{x}_j^{(0)} - \hat{\mathbf{z}}_m^{(1)}).$$

The gradient of  $\mathcal{L}^{(1)}$  w.r.t.  $w_{j,m}^{(1)}$  is

$$\frac{\partial \mathcal{L}^{(1)}}{\partial w_{j,m}^{(1)}} = \frac{\sigma_j(\mathbf{w}_m^{(1)})}{B} \langle \mathbf{P}_1^\top (\mathbf{P}_1 \phi(\hat{\mathbf{z}}_m^{(1)}) - \mathbf{b}_m), \phi'(\hat{\mathbf{z}}_m^{(1)}), \mathbf{x}_j^{(0)} - \hat{\mathbf{z}}_m^{(1)} \rangle.$$

At initialization  $\mathbf{W}^{(1)} = 0$ ,  $\sigma_j(\mathbf{w}_m^{(1)}) = 1/n$  for  $j \in [n]$  and 0 otherwise. Expanding  $\phi$  and  $\phi'$  around 0 via  $\phi(t) = -1 + ct^2 + O(t^4)$ ,  $\phi'(t) = 2ct + O(t^3)$ ,

$$\frac{\partial \mathcal{L}^{(1)}}{\partial w_{j,m}^{(1)}} = \frac{1}{nB} \left( - \langle \mathbf{P}_1^\top \mathbf{b}_m, 2c\hat{\mathbf{z}}_m, \mathbf{x}_j - \hat{\mathbf{z}}_m \rangle \right) \quad (3)$$

$$+ \langle \mathbf{P}_1^\top \mathbf{P}_1(-\mathbf{1}_d + c\hat{\mathbf{z}}_m^2), 2c\hat{\mathbf{z}}_m, \mathbf{x}_j - \hat{\mathbf{z}}_m \rangle \quad (4)$$

$$+ \langle O(\mathbf{P}_1^\top \mathbf{P}_1 |\hat{\mathbf{z}}_m|^4), 2c\hat{\mathbf{z}}_m, \mathbf{x}_j - \hat{\mathbf{z}}_m \rangle \quad (5)$$

$$+ \langle \mathbf{P}_1^\top (\mathbf{P}_1 \phi(\hat{\mathbf{z}}_m) - \mathbf{b}_m), O(|\hat{\mathbf{z}}_m|^3), \mathbf{x}_j - \hat{\mathbf{z}}_m \rangle \Big). \quad (6)$$

**Signal term (3).** Substituting  $\hat{\mathbf{z}}_m = \frac{1}{n} \sum_{\alpha \in [n]} \mathbf{x}_\alpha$ ,

$$\begin{aligned} & \frac{1}{B} \langle \mathbf{P}_1^\top \mathbf{b}_m, \hat{\mathbf{z}}_m, \mathbf{x}_j - \hat{\mathbf{z}}_m \rangle \\ &= \frac{1}{nB} \left( \sum_{\alpha \in [n]} \langle \mathbf{b}_m, \mathbf{x}_{\alpha,[1]}, \mathbf{x}_{j,[1]} \rangle - \frac{1}{n} \sum_{\alpha, \beta \in [n]} \langle \mathbf{b}_m, \mathbf{x}_{\alpha,[1]}, \mathbf{x}_{\beta,[1]} \rangle \right). \end{aligned}$$

Since  $\mathbf{P}_1^\top \mathbf{b}_m$  is supported on block 1 only and  $\mathbf{x}_{\alpha,[1]} = \mathbf{b}_\alpha$  at stage 1's input,

$$\langle \mathbf{P}_1^\top \mathbf{b}_m, \mathbf{x}_\alpha, \mathbf{x}_\beta \rangle = \langle \mathbf{b}_m, \mathbf{b}_\alpha, \mathbf{b}_\beta \rangle.$$

The customized mask restricts  $\alpha, \beta$  to  $[n]$ , so  $h[\alpha] = h[\beta] = 1$ . By the parity tree's structure,  $\mathbf{b}_m$  at level  $h[m] = 2$  covers two disjoint input bits, namely  $\mathbf{b}_{c_1[m]}$  and  $\mathbf{b}_{c_2[m]}$ . For  $\langle \mathbf{b}_m, \mathbf{b}_\alpha, \mathbf{b}_\beta \rangle$  to be trivial,  $\mathbf{b}_\alpha \odot \mathbf{b}_\beta = \mathbf{b}_m$ , which holds iff  $\{\alpha, \beta\} = \{c_1[m], c_2[m]\}$ . For non-trivial tuples, Lemma 5 gives  $|\langle \mathbf{b}_m, \mathbf{b}_\alpha, \mathbf{b}_\beta \rangle| \leq B\kappa$  where  $\kappa = O(n^{-1-\epsilon/4})$ . Combining,

$$\frac{1}{B} \sum_{\alpha, \beta \in [n]} \langle \mathbf{b}_m, \mathbf{b}_\alpha, \mathbf{b}_\beta \rangle = 2 + O(n^2\kappa).$$

Similarly,  $\langle \mathbf{b}_m, \mathbf{b}_\alpha, \mathbf{b}_j \rangle$  is non-trivial only when  $p[j] = m$  and  $\alpha$  is the other child of  $m$ . As a result,

$$\frac{1}{B} \sum_{\alpha \in [n]} \langle \mathbf{b}_m, \mathbf{b}_\alpha, \mathbf{b}_j \rangle = \begin{cases} 1 + O(n\kappa) & p[j] = m, \\ O(n\kappa) & \text{otherwise.} \end{cases}$$

Combining,

$$-\frac{1}{nB} \langle \mathbf{P}_1^\top \mathbf{b}_m, 2c\hat{\mathbf{z}}_m, \mathbf{x}_j - \hat{\mathbf{z}}_m \rangle = -\frac{2c}{n^2} \mathbb{1}(p[j] = m) + O(n^{-2-\epsilon/4}).$$

Next for Eq. (4), we write

$$\begin{aligned} & \frac{1}{B} \langle \mathbf{P}_1^\top \mathbf{P}_1(-\mathbf{1}_d + c\hat{\mathbf{z}}_m^2), 2c\hat{\mathbf{z}}_m, \mathbf{x}_j - \hat{\mathbf{z}}_m \rangle \\ &= -\frac{2c}{B} \langle \hat{\mathbf{z}}_{m,[1]}, \mathbf{x}_{j,[1]} \rangle + \frac{2c}{B} \langle \hat{\mathbf{z}}_{m,[1]}^2 \rangle + \frac{2c^2}{B} \langle \hat{\mathbf{z}}_{m,[1]}^3, \mathbf{x}_{j,[1]} \rangle - \frac{2c^2}{B} \langle \hat{\mathbf{z}}_{m,[1]}^4 \rangle. \end{aligned}$$

For the second-order terms, we have:

$$\begin{aligned} \frac{1}{B} \langle \hat{\mathbf{z}}_{m,[1]}, \mathbf{x}_{j,[1]} \rangle &= \frac{1}{nB} \left( \langle \mathbf{b}_j, \mathbf{b}_j \rangle + \sum_{\alpha \neq j, \alpha \in [n]} \langle \mathbf{b}_\alpha, \mathbf{b}_j \rangle \right) = \frac{1}{n} + O(\kappa), \\ \frac{1}{B} \langle \hat{\mathbf{z}}_{m,[1]}^2 \rangle &= \frac{1}{n^2 B} \left( \sum_{\alpha \in [n]} \langle \mathbf{b}_\alpha, \mathbf{b}_\alpha \rangle + \sum_{\alpha \neq \beta, \alpha, \beta \in [n]} \langle \mathbf{b}_\alpha, \mathbf{b}_\beta \rangle \right) = \frac{1}{n} + O(\kappa). \end{aligned}$$

For the fourth-order interaction terms, we discuss when  $(\alpha, \beta, \gamma, \delta) \notin I_{4,m}$ . By Lemma 6, the total count of trivial 4-tuples is  $O(n^2)$ . Therefore,

$$\begin{aligned} \frac{1}{B} \langle \hat{\mathbf{z}}_{m,[1]}^4 \rangle &= \frac{1}{n^4 B} \sum_{\alpha, \beta, \gamma, \delta \in [n]} \langle \mathbf{b}_\alpha, \mathbf{b}_\beta, \mathbf{b}_\gamma, \mathbf{b}_\delta \rangle \\ &= \frac{1}{n^4 B} \left( \sum_{\alpha, \beta, \gamma, \delta \in I_{4,m}} O(B\kappa) + \sum_{\alpha, \beta, \gamma, \delta \notin I_{4,m}} B \right) \\ &\leq \frac{1}{n^4} (O(n^2) + n^4 \kappa) \\ &= O(n^{-2} + \kappa). \end{aligned}$$

Now for  $\langle \hat{\mathbf{z}}_{m,[1]}^3, \mathbf{x}_{j,[1]} \rangle$ , assuming index  $j$  is contained in  $(\alpha, \beta, \gamma, \delta)$ . Then case 1 in Lemma 6 has  $O(1)$  trivial tuples, cases 3 and 4 are reduced to  $O(n)$  (one free index). Thus

$$\frac{1}{B} \langle \hat{\mathbf{z}}_{m,[1]}^3, \mathbf{x}_{j,[1]} \rangle = \frac{1}{n^3 B} \sum_{\alpha, \beta, \gamma \in [n]} \langle \mathbf{b}_\alpha, \mathbf{b}_\beta, \mathbf{b}_\gamma, \mathbf{b}_j \rangle \leq O(n^{-2} + \kappa).$$

Combining,

$$\frac{1}{nB} \langle \mathbf{P}_1^\top \mathbf{P}_1 (-\mathbf{1}_d + c\hat{\mathbf{z}}_m^2), 2c\hat{\mathbf{z}}_m, \mathbf{x}_j - \hat{\mathbf{z}}_m \rangle = \frac{O(\kappa)}{n} = O(n^{-2-\epsilon/4}).$$

For Eq. (5), note that

$$\frac{1}{B} \langle \mathbf{P}_1^\top \mathbf{P}_1 |\hat{\mathbf{z}}_m|^4 \rangle = \frac{1}{B} \langle \hat{\mathbf{z}}_{m,[1]}^4 \rangle = O(n^{-2} + \kappa),$$

and since  $2c\hat{\mathbf{z}}_m, \mathbf{x}_j - \hat{\mathbf{z}}_m$  are contained in  $[-1, 1]$  and  $[-2, 2]$  respectively,

$$\frac{1}{nB} \langle O(\mathbf{P}_1^\top \mathbf{P}_1 |\hat{\mathbf{z}}_m|^4), 2c\hat{\mathbf{z}}_m, \mathbf{x}_j - \hat{\mathbf{z}}_m \rangle = \frac{4c}{n} O(n^{-2} + \kappa) = O(n^{-2-\epsilon/4}).$$

Finally for Eq. (6), by Cauchy-Schwarz,

$$\begin{aligned} \frac{1}{B} \langle \mathbf{P}_1^\top \mathbf{P}_1 |\hat{\mathbf{z}}_m|^3 \rangle &= \frac{1}{B} \sum_{i=1}^B |\hat{\mathbf{z}}_{m,[1],i}^3| \leq \frac{1}{B} \left( \sum_{i=1}^B \hat{\mathbf{z}}_{m,[1],i}^2 \right)^{1/2} \left( \sum_{i=1}^B \hat{\mathbf{z}}_{m,[1],i}^4 \right)^{1/2} \\ &= O(n^{-1-\epsilon/8}). \end{aligned}$$

By the definition of  $\mathbf{P}_1$ ,

$$\begin{aligned} &\frac{1}{nB} \langle \mathbf{P}_1^\top (\mathbf{P}_1 \phi(\hat{\mathbf{z}}_m) - \mathbf{b}_m), O(|\hat{\mathbf{z}}_m|^3), \mathbf{x}_j - \hat{\mathbf{z}}_m \rangle \\ &= \frac{1}{nB} \langle \phi(\hat{\mathbf{z}}_m) - \mathbf{P}_1^\top \mathbf{b}_m, O(\mathbf{P}_1^\top \mathbf{P}_1 |\hat{\mathbf{z}}_m|^3), \mathbf{x}_j - \hat{\mathbf{z}}_m \rangle \\ &= \frac{4}{nB} \langle O(\mathbf{P}_1^\top \mathbf{P}_1 |\hat{\mathbf{z}}_m|^3) \rangle \\ &= O(n^{-2-\epsilon/8}). \end{aligned}$$

Combining all terms from (3) to (6), for any  $j \in [n]$ , we get

$$\frac{\partial \mathcal{L}^{(1)}}{\partial w_{j,m}^{(1)}} = -\frac{2c}{n^2} \mathbb{1}(p[j] = m) + O(n^{-2-\epsilon/8}).$$

Note that this applies to the approximate gradient  $\tilde{\nabla}_{w_{j,m}^{(1)}} \mathcal{L}^{(1)}$  too since each component of the noise is bounded by  $O(n^{-2-\epsilon/8})$ .

**Concentration of attention scores at  $m \in [n+1, n_2]$ .** The gradient above has a signal of order  $n^{-2}$  and a noise remainder of order  $n^{-2-\epsilon/8}$ . For the integer quantization  $q(\cdot)$  to map both children's updates to the same integer while rounding non-child noise to zero, the leading term must land near an integer with margin exceeding the post-scaling noise. Under the customized mask in Figure 2(a), every query  $m \in [n+1, n_2]$  shares the same signal prefactor  $n^{-2}$ , so we use a stage-wise learning rate

$$\eta_1 := \frac{K_n n^2}{2c}, \quad K_n := \lceil n^{\epsilon/16} \rceil,$$

where  $c > 0$  is the link function constant from Definition 2. This design cancels the prefactor exactly and scales the signal to  $K_n$ . The update for  $m \in [n+1, n_2]$  becomes

$$w_{j,m}^{(1)}(1) = q(K_n \mathbb{1}(p[j] = m) + \Delta_{j,m}), \quad (7)$$

where  $\Delta_{j,m} := \eta_1 R_{j,m}$  and the noise term  $R_{j,m}$  satisfies  $|R_{j,m}| \leq C_{\nabla} n^{-2-\epsilon/8}$  uniformly. Since  $K_n \leq 2n^{\epsilon/16}$  for sufficiently large  $n$ ,

$$|\Delta_{j,m}| \leq \frac{K_n n^2}{2c} \cdot C_{\nabla} n^{-2-\epsilon/8} \leq C'_{\nabla} n^{-\epsilon/16} < \frac{1}{2}.$$

*Non-children indices.* For  $j \notin \{c_1[m], c_2[m]\}$ , the indicator  $\mathbb{1}(p[j] = m)$  vanishes, so  $w_{j,m}^{(1)}(1) = q(\Delta_{j,m}) = 0$ .

*Children indices.* For  $j \in \{c_1[m], c_2[m]\}$ , since  $K_n \in \mathbb{Z}$  and  $|\Delta_{j,m}| < 1/2$ ,

$$w_{j,m}^{(1)}(1) = q(K_n + \Delta_{j,m}) = K_n.$$

Thus  $w_{c_1[m],m}^{(1)}(1) = w_{c_2[m],m}^{(1)}(1) = K_n$ , while all non-child logits are zero.

*Softmax concentration.* The total softmax mass on non-child indices is bounded by

$$\sum_{j \notin \{c_1[m], c_2[m]\}} \sigma_j(\mathbf{w}_m^{(1)}) \leq \frac{n-2}{2e^{K_n} + (n-2)} \leq ne^{-K_n} \leq \exp(-Cn^{\epsilon/16})$$

for some constant  $C > 0$  and sufficiently large  $n$ . Since the two child logits are exactly equal,

$$\frac{1 - \exp(-Cn^{\epsilon/16})}{2} \leq \sigma_{c_1[m]}(\mathbf{w}_m^{(1)}) = \sigma_{c_2[m]}(\mathbf{w}_m^{(1)}) \leq \frac{1}{2}.$$

**Forward pass evaluation at  $m \in [n+1, n_2]$ .** For  $m \in [n+1, n_2]$ , the children  $c_1[m], c_2[m]$  are at level 1 (input bits), so  $\mathbf{x}_{c_i[m],1}^{(0)} = \mathbf{b}_{c_i[m]}$  exactly. Hence

$$\begin{aligned} \left\| \hat{\mathbf{z}}_{m,[1]}^{(1)} - \frac{\mathbf{b}_{c_1[m]} + \mathbf{b}_{c_2[m]}}{2} \right\|_{\infty} &\leq \sum_{p[j] \neq m} \sigma_j(\mathbf{w}_m^{(1)}) + \left| \sigma_{c_1[m]}(\mathbf{w}_m^{(1)}) - \frac{1}{2} \right| + \left| \sigma_{c_2[m]}(\mathbf{w}_m^{(1)}) - \frac{1}{2} \right| \\ &\leq 2 \exp(-Cn^{\epsilon/16}). \end{aligned}$$

By Taylor expansion of  $\phi$  around

$$s_m := \frac{b_{c_1[m]} + b_{c_2[m]}}{2} \in \{-1, 0, 1\},$$

using

$$\phi(s_m) = b_{c_1[m]} b_{c_2[m]} = b_m \quad \text{and} \quad \phi'(s_m) = 0,$$

we obtain

$$\begin{aligned} \|\mathbf{x}_{m,[2]}^{(1)} - \mathbf{b}_m\|_\infty &= \left\| \phi(\hat{\mathbf{z}}_{m,[1]}^{(1)}) - \phi\left(\frac{\mathbf{b}_{c_1[m]} + \mathbf{b}_{c_2[m]}}{2}\right) \right\|_\infty \\ &\leq C_2(2\exp(-Cn^{\epsilon/16}))^2 \leq \exp(-Cn^{\epsilon/16}). \end{aligned} \quad (8)$$

□

At each stage  $t \geq 1$ , we replace the first  $k(1 - 2^{-(t-1)})$  thinking tokens with padding tokens. This ensures that at  $L := \log_2 k$  stages, we are relying only on the input bits to predict. The input sequence looks like

$$\mathbf{b}^{(t)} = (\mathbf{b}_1, \dots, \mathbf{b}_n, \underbrace{\mathbf{0}_B, \dots, \mathbf{0}_B}_{n_t - n}, \mathbf{b}_{n_t+1}, \mathbf{b}_{n_t+2}, \dots, \mathbf{b}_T)$$

The loss function is only computed on position  $n_t + 1 \leq m \leq T$ , i.e.,

$$\mathcal{L}^{(t)}(\boldsymbol{\theta}) = \frac{1}{2B} \sum_{m=n_t+1}^T \|\hat{f}(\mathbf{D})_m - \mathbf{b}_m\|^2$$

At training time, since the first  $k(1 - 2^{-(t-1)})$  thinking tokens are masked, the model needs to rely on the hidden thinking traces in  $t$ -th layer to do the prediction for  $n_t + 1 \leq m \leq n_{t+1}$ . Similar to the first stage, we can learn the  $t$ -th layer by one step of gradient descent as shown in Lemma 9. Before proceeding, we first state a lemma that characterizes how the hidden states progress over layers.

**Lemma 8** (Characterization of Hidden States at Stage  $s$ ). *Fix a curriculum stage  $s \in [L]$ . Suppose that for all  $\tau \in \{1, \dots, s-1\}$ , the per-layer recursion satisfies*

$$\mathbf{x}_{m, [\tau+1]}^{(\tau)} = \begin{cases} \mathbf{b}_m + \boldsymbol{\xi}, & n_\tau + 1 \leq m \leq n_{\tau+1}, \\ \mathbf{x}_{m, [\tau]}^{(\tau-1)}, & \text{otherwise,} \end{cases} \quad (9)$$

where  $\|\boldsymbol{\xi}\|_\infty \leq \delta := \exp(-Cn^{\epsilon/16})$ . Then for any layer  $\ell \in \{0, 1, \dots, s-1\}$  and any  $\beta \in [T]$ ,

$$\mathbf{x}_{\beta, [\ell+1]}^{(\ell)} = \begin{cases} \mathbf{b}_\beta + \boldsymbol{\xi}, & n + 1 \leq \beta \leq n_{\ell+1}, \\ \mathbf{b}_\beta, & \beta \leq n \text{ or } \beta > n_s, \\ \mathbf{0}_B, & n_{\ell+1} < \beta \leq n_s, \end{cases} \quad (10)$$

*Proof.* We prove Eq. (10) by induction on  $\ell$ .

**Base case ( $\ell = 0$ ).** At  $\ell = 0$ , the residual stream is the curriculum's stage- $s$  input:

$$\mathbf{x}_{\beta, [1]}^{(0)} = \begin{cases} \mathbf{b}_\beta, & \beta \leq n \text{ or } \beta > n_s, \\ \mathbf{0}_B, & n + 1 \leq \beta \leq n_s. \end{cases}$$

Since  $n_{\ell+1} = n_1 = n$ , the ‘‘computed’’ range  $n + 1 \leq \beta \leq n_{\ell+1}$  is empty, and the three cases above coincide with the three cases of Eq. (10) at  $\ell = 0$ .

**Inductive step** ( $\ell \Rightarrow \ell + 1$ , for  $\ell + 1 \leq s - 1$ ). Assume Eq. (10) holds at layer  $\ell$ . We verify it at layer  $\ell + 1$  by partitioning  $[T]$  into two regions and applying Eq. (9) at  $\tau = \ell + 1$ :

**Region 1: Newly computed positions** ( $n_{\ell+1} + 1 \leq \beta \leq n_{\ell+2}$ ). By Eq. (9),

$$\mathbf{x}_{\beta, [\ell+2]}^{(\ell+1)} = \mathbf{b}_\beta + \boldsymbol{\xi}, \quad \|\boldsymbol{\xi}\|_\infty \leq \delta.$$

Since  $n + 1 \leq \beta \leq n_{\ell+2}$ , this matches the computed-range case of Eq. (10) at  $\ell + 1$ .

**Region 2: Inherited positions** ( $\beta \leq n_{\ell+1}$  or  $\beta > n_{\ell+2}$ ). For these positions, Eq. (9) gives  $\mathbf{x}_{\beta, [\ell+2]}^{(\ell+1)} = \mathbf{x}_{\beta, [\ell+1]}^{(\ell)}$ , so the value is inherited from layer  $\ell$  and we apply the inductive hypothesis:

- If  $n + 1 \leq \beta \leq n_{\ell+1}$  (previously computed), then  $\mathbf{x}_{\beta, [\ell+1]}^{(\ell)} = \mathbf{b}_\beta + \boldsymbol{\xi}$  with  $\|\boldsymbol{\xi}\|_\infty \leq \delta$ . Since  $\beta \in [n + 1, n_{\ell+2}]$ , this matches the computed-range case at  $\ell + 1$ .
- If  $\beta \leq n$  or  $\beta > n_s$  (shown), then  $\mathbf{x}_{\beta, [\ell+1]}^{(\ell)} = \mathbf{b}_\beta$ , matching the shown-range case at  $\ell + 1$ .
- If  $n_{\ell+2} < \beta \leq n_s$  (padded), then  $\beta$  also satisfies  $n_{\ell+1} < \beta \leq n_s$ , so by the inductive hypothesis  $\mathbf{x}_{\beta, [\ell+1]}^{(\ell)} = \mathbf{0}_B$ , matching the padded-range case at  $\ell + 1$ .

In both regions, Eq. (10) holds at layer  $\ell + 1$ . This completes the induction.  $\square$

**Lemma 9** (Inductive Step). *Fix any  $t \in \{1, \dots, L - 1\}$ . Suppose layers  $1, \dots, t$  are well-trained (Definition 4) and  $\mathbf{W}^{(\ell)}(t) = \mathbf{0}$  for all  $\ell \geq t + 1$ . After one gradient step on the stage- $(t + 1)$  loss  $\mathcal{L}^{(t+1)}$  with  $B$  training samples and stage-wise learning rate  $\eta_{t+1} = K_n n_{t+1}^2 / (2c)$ , where  $B = \Omega(n^{2+\epsilon})$ ,  $K_n := \lceil n^{\epsilon/16} \rceil$  and  $c > 0$  is the link function constant in Definition 2, with probability  $1 - \exp(-n^{\epsilon/2})$  over the fresh stage- $(t + 1)$  batch, layer  $t + 1$  is also well-trained (Definition 4).*

*Proof.* By the assumption that layers  $1, \dots, t$  are well-trained and Lemma 8 (applied with  $s = t + 1$ ,  $\ell = t$ ), the hidden states satisfy  $\mathbf{x}_{\tau, [t+1]}^{(t)} = \mathbf{b}_\tau + \boldsymbol{\xi}$  with  $\|\boldsymbol{\xi}\|_\infty \leq \delta = \exp(-Cn^{\epsilon/16})$  for all  $\tau \in [T]$ . Recall that

$$\begin{aligned} & \mathcal{L}^{(t+1)}(\boldsymbol{\theta}) \\ &= \frac{1}{2B} \sum_{m=n_{t+1}+1}^T \|\Psi_{t+1}^\top \mathbf{W}_O^{(t+1)} \left( g_m^{(t+1)} \phi \left( \sum_{j=1}^{n_{h[m]}-1} \sigma_j(\mathbf{w}_m^{(t+1)}) \mathbf{x}_j^{(t)} \right) + (1 - g_m^{(t+1)}) \mathbf{x}_m^{(t)} \right) - \mathbf{b}_m \|^2. \end{aligned}$$

We split into two cases.

**Case 1:**  $m \in [n_{t+1} + 1, n_{t+2}]$ . Here  $g_m^{(t+1)} = 1$  (active) and the gradient encodes a non-trivial signal from the contraction.

**Case 2:**  $m > n_{t+2}$ . Here  $g_m^{(t+1)} = 0$  by per-block gating, layer  $t + 1$  does not write at position  $m$ , and the gradient is identically zero. We treat case 1 in detail and then briefly address case 2 at the end of the proof.

**Case 1:**  $m \in [n_{t+1} + 1, n_{t+2}]$ . Under the causal mask,  $\sigma_j(\mathbf{w}_m) = 1/n_{t+1}$  for  $j \in [n_{t+1}]$  and 0

otherwise at initialization  $\mathbf{W}^{(t+1)} = 0$ .

$$\begin{aligned} \frac{\partial \mathcal{L}^{(t+1)}}{\partial w_{j,m}^{(t+1)}} &= \frac{\sigma_j(\mathbf{w}_m^{(t+1)})}{B} \langle \mathbf{P}_{t+1}^\top (\mathbf{P}_{t+1} \phi(\hat{\mathbf{z}}_m^{(t+1)}) - \mathbf{b}_m), \phi'(\hat{\mathbf{z}}_m^{(t+1)}), \mathbf{x}_j^{(t)} - \hat{\mathbf{z}}_m^{(t+1)} \rangle \\ &= -\frac{1}{n_{t+1}B} \langle \mathbf{P}_{t+1}^\top \mathbf{b}_m, 2c\hat{\mathbf{z}}_m^{(t+1)}, \mathbf{x}_j^{(t)} - \hat{\mathbf{z}}_m^{(t+1)} \rangle \end{aligned} \quad (11)$$

$$+ \frac{1}{n_{t+1}B} \langle \mathbf{P}_{t+1}^\top \mathbf{P}_{t+1} (-\mathbf{1}_d + c(\hat{\mathbf{z}}_m^{(t+1)})^2), 2c\hat{\mathbf{z}}_m^{(t+1)}, \mathbf{x}_j^{(t)} - \hat{\mathbf{z}}_m^{(t+1)} \rangle \quad (12)$$

$$+ \frac{1}{n_{t+1}B} \langle O(\mathbf{P}_{t+1}^\top \mathbf{P}_{t+1} |\hat{\mathbf{z}}_m^{(t+1)}|^4), 2c\hat{\mathbf{z}}_m^{(t+1)}, \mathbf{x}_j^{(t)} - \hat{\mathbf{z}}_m^{(t+1)} \rangle \quad (13)$$

$$+ \frac{1}{n_{t+1}B} \langle \mathbf{P}_{t+1}^\top (\mathbf{P}_{t+1} \phi(\hat{\mathbf{z}}_m^{(t+1)}) - \mathbf{b}_m), O(|\hat{\mathbf{z}}_m^{(t+1)}|^3), \mathbf{x}_j^{(t)} - \hat{\mathbf{z}}_m^{(t+1)} \rangle. \quad (14)$$

For Equation (11), we substitute  $\hat{\mathbf{z}}_m^{(t+1)} = \frac{1}{n_{t+1}} \sum_{\alpha \in [n_{t+1}]} \mathbf{x}_\alpha^{(t)}$  to expand

$$\begin{aligned} &\frac{1}{B} \langle \mathbf{P}_{t+1}^\top \mathbf{b}_m, \hat{\mathbf{z}}_m^{(t+1)}, \mathbf{x}_j^{(t)} - \hat{\mathbf{z}}_m^{(t+1)} \rangle \\ &= \frac{1}{n_{t+1}B} \left( \sum_{\alpha \in [n_{t+1}]} \langle \mathbf{b}_m, \mathbf{x}_{\alpha, [t+1]}^{(t)}, \mathbf{x}_{j, [t+1]}^{(t)} \rangle - \frac{1}{n_{t+1}} \sum_{\alpha, \beta \in [n_{t+1}]} \langle \mathbf{b}_m, \mathbf{x}_{\alpha, [t+1]}^{(t)}, \mathbf{x}_{\beta, [t+1]}^{(t)} \rangle \right). \end{aligned}$$

The customized mask restricts  $\alpha, \beta$  to  $[n_{t+1}]$ , so  $h[\alpha], h[\beta] \leq t+1 < h[m] = t+2$ . By the parity tree's structure, distinct same-level nodes cover disjoint subsets of input bits, and  $\mathbf{b}_m$  covers  $2^{t+1}$  disjoint input bits at level  $t+2$ . For  $\langle \mathbf{b}_m, \mathbf{b}_\alpha, \mathbf{b}_\beta \rangle$  to be trivial, the bit multiplicities must align, which forces  $\mathbf{b}_\alpha \odot \mathbf{b}_\beta = \mathbf{b}_m$ , i.e.,  $\{\alpha, \beta\} = \{c_1[m], c_2[m]\}$  at level  $t+1$ . Hence,

$$\left| \langle \mathbf{b}_m, \mathbf{x}_{\alpha, [t+1]}^{(t)}, \mathbf{x}_{\beta, [t+1]}^{(t)} \rangle \right| \leq |\langle \mathbf{b}_m, \mathbf{b}_\alpha, \mathbf{b}_\beta \rangle| + 2\delta B + \delta^2 B = B(1 + O(\delta)),$$

and for non-trivial  $(\alpha, \beta)$ ,

$$\left| \langle \mathbf{b}_m, \mathbf{x}_{\alpha, [t+1]}^{(t)}, \mathbf{x}_{\beta, [t+1]}^{(t)} \rangle \right| \leq B\kappa + 2\delta B + \delta^2 B = O(B(\kappa + \delta)).$$

Using  $n_{t+1} = \Theta(n)$  (specifically  $n \leq n_{t+1} < 2n$ ), putting these together,

$$\frac{1}{B} \sum_{\alpha, \beta \in [n_{t+1}]} \langle \mathbf{b}_m, \mathbf{x}_{\alpha, [t+1]}^{(t)}, \mathbf{x}_{\beta, [t+1]}^{(t)} \rangle = 2 + O(n^2\delta) + O(n^2\kappa) = 2 + O(n^2\kappa).$$

Similarly,  $\langle \mathbf{b}_m, \mathbf{x}_{\alpha, [t+1]}^{(t)}, \mathbf{x}_{j, [t+1]}^{(t)} \rangle$  is non-trivial only when  $p[j] = m$  and  $\alpha$  is the other child. By the same expansion,

$$\frac{1}{B} \sum_{\alpha \in [n_{t+1}]} \langle \mathbf{b}_m, \mathbf{x}_{\alpha, [t+1]}^{(t)}, \mathbf{x}_{j, [t+1]}^{(t)} \rangle = \begin{cases} 1 + O(n\kappa) & p[j] = m, \\ O(n\kappa) & \text{o.w.} \end{cases}$$

Combining these with  $\kappa = O(n^{-1-\epsilon/4})$ ,

$$-\frac{1}{n_{t+1}B} \langle \mathbf{P}_{t+1}^\top \mathbf{b}_m, 2c\hat{\mathbf{z}}_m^{(t+1)}, \mathbf{x}_j^{(t)} - \hat{\mathbf{z}}_m^{(t+1)} \rangle = -\frac{2c}{n_{t+1}^2} \mathbb{1}[p[j] = m] + O(n^{-2-\epsilon/4}).$$

Next for Equation (12), we expand

$$\begin{aligned} & \frac{1}{B} \langle \mathbf{P}_{t+1}^\top \mathbf{P}_{t+1} (-\mathbf{1}_d + c(\hat{\mathbf{z}}_m^{(t+1)})^2), 2c\hat{\mathbf{z}}_m^{(t+1)}, \mathbf{x}_j^{(t)} - \hat{\mathbf{z}}_m^{(t+1)} \rangle \\ &= -\frac{2c}{B} \langle \hat{\mathbf{z}}_{m,[t+1]}^{(t+1)}, \mathbf{x}_{j,[t+1]}^{(t)} \rangle + \frac{2c}{B} \langle (\hat{\mathbf{z}}_{m,[t+1]}^{(t+1)})^2 \rangle + \frac{2c^2}{B} \langle (\hat{\mathbf{z}}_{m,[t+1]}^{(t+1)})^3, \mathbf{x}_{j,[t+1]}^{(t)} \rangle - \frac{2c^2}{B} \langle (\hat{\mathbf{z}}_{m,[t+1]}^{(t+1)})^4 \rangle. \end{aligned}$$

For the second-order terms, we have:

$$\begin{aligned} \frac{1}{B} \langle \hat{\mathbf{z}}_{m,[t+1]}^{(t+1)}, \mathbf{x}_{j,[t+1]}^{(t)} \rangle &= \frac{1}{n_{t+1}B} \left( \langle \mathbf{x}_{j,[t+1]}^{(t)}, \mathbf{x}_{j,[t+1]}^{(t)} \rangle + \sum_{\alpha \neq j, \alpha \in [n_{t+1}]} \langle \mathbf{x}_{\alpha,[t+1]}^{(t)}, \mathbf{x}_{j,[t+1]}^{(t)} \rangle \right) \\ &= \frac{1}{n_{t+1}B} \left( \langle \mathbf{b}_j, \mathbf{b}_j \rangle + \sum_{\alpha \neq j} \langle \mathbf{b}_\alpha, \mathbf{b}_j \rangle \right) + \frac{O(n)}{n_{t+1}} (\delta + \delta^2) \\ &= \frac{1}{n_{t+1}} (1 + (n_{t+1} - 1)\kappa) + \frac{O(n)}{n_{t+1}} (\delta + \delta^2) \\ &= \frac{1}{n_{t+1}} + O(\kappa). \end{aligned}$$

Similarly,

$$\begin{aligned} \frac{1}{B} \langle (\hat{\mathbf{z}}_{m,[t+1]}^{(t+1)})^2 \rangle &= \frac{1}{n_{t+1}^2 B} \left( \sum_{\alpha} \langle \mathbf{x}_{\alpha,[t+1]}^{(t)}, \mathbf{x}_{\alpha,[t+1]}^{(t)} \rangle + \sum_{\alpha \neq \beta} \langle \mathbf{x}_{\alpha,[t+1]}^{(t)}, \mathbf{x}_{\beta,[t+1]}^{(t)} \rangle \right) \\ &= \frac{1}{n_{t+1}^2 B} \left( \sum_{\alpha} \langle \mathbf{b}_\alpha, \mathbf{b}_\alpha \rangle + \sum_{\alpha \neq \beta} \langle \mathbf{b}_\alpha, \mathbf{b}_\beta \rangle \right) + \frac{O(n)}{n_{t+1}} \delta + \frac{O(n^2)}{n_{t+1}^2} \delta^2 \\ &= \frac{1}{n_{t+1}} + O(\kappa). \end{aligned}$$

For the fourth-order interaction terms, we discuss when  $(\alpha, \beta, \gamma, \delta) \notin I_{4,m}$ , i.e.,  $\langle \mathbf{b}_\alpha, \mathbf{b}_\beta, \mathbf{b}_\gamma, \mathbf{b}_\delta \rangle$  is trivial. Again, by the bit-counting argument in Lemma 6, the number of trivial ones are at most  $O(n^2)$ . Hence,

$$\begin{aligned} \frac{1}{B} \langle (\hat{\mathbf{z}}_{m,[t+1]}^{(t+1)})^4 \rangle &= \frac{1}{n_{t+1}^4 B} \sum_{\alpha, \beta, \gamma, \delta \in [n_{t+1}]} \langle \mathbf{x}_{\alpha,[t+1]}^{(t)}, \mathbf{x}_{\beta,[t+1]}^{(t)}, \mathbf{x}_{\gamma,[t+1]}^{(t)}, \mathbf{x}_{\delta,[t+1]}^{(t)} \rangle \\ &= \frac{1}{n_{t+1}^4 B} \sum_{\alpha, \beta, \gamma, \delta \in [n_{t+1}]} \langle \mathbf{b}_\alpha, \mathbf{b}_\beta, \mathbf{b}_\gamma, \mathbf{b}_\delta \rangle + \sum_{j=1}^3 \frac{O(n^j)}{n_{t+1}^j} \delta^j \kappa + \frac{O(n^4)}{n_{t+1}^4} \delta^4 \\ &\leq \frac{1}{n_{t+1}^4 B} \left( \sum_{\alpha, \beta, \gamma, \delta \in I_{4,m}} O(B\kappa) + \sum_{\alpha, \beta, \gamma, \delta \notin I_{4,m}} B \right) + O(\delta) \\ &\leq \frac{1}{n_{t+1}^4} (O(n^2) + n_{t+1}^4 \kappa) + O(\delta) \\ &= O(n^{-2} + \kappa). \end{aligned}$$

Now for  $\langle (\hat{\mathbf{z}}_{m,[t+1]}^{(t+1)})^3, \mathbf{x}_{j,[t+1]}^{(t)} \rangle$ , assuming index  $j$  is contained in  $(\alpha, \beta, \gamma, \delta)$ . Repeating the argument

in Lemma 7, we get

$$\begin{aligned}
\frac{1}{B} \langle (\hat{\mathbf{z}}_{m,[t+1]}^{(t+1)})^3, \mathbf{x}_{j,[t+1]}^{(t)} \rangle &\leq \frac{1}{n_{t+1}^3 B} \sum_{\alpha, \beta, \gamma \in [n_{t+1}]} \langle \mathbf{b}_\alpha, \mathbf{b}_\beta, \mathbf{b}_\gamma, \mathbf{b}_j \rangle + O(n^{-1-\epsilon/4}) \\
&\leq \frac{1}{n_{t+1}^3} (O(n) + n_{t+1}^3 \kappa) + O(\delta) \\
&= O(n^{-2} + \kappa).
\end{aligned}$$

For Eq. (13), note that

$$\frac{1}{B} \langle \mathbf{P}_{t+1}^\top \mathbf{P}_{t+1} |\hat{\mathbf{z}}_m^{(t+1)}|^4 \rangle = \frac{1}{B} \langle |\hat{\mathbf{z}}_{m,[t+1]}^{(t+1)}|^4 \rangle = \frac{1}{B} \langle (\hat{\mathbf{z}}_{m,[t+1]}^{(t+1)})^4 \rangle = O(n^{-2} + \kappa).$$

and since  $2c\hat{\mathbf{z}}_m^{(t+1)}, \mathbf{x}_j^{(t)} - \hat{\mathbf{z}}_m^{(t+1)}$  are contained in  $[-1, 1]$  and  $[-2, 2]$  respectively. We have

$$\frac{1}{n_{t+1} B} \langle \mathbf{P}_{t+1}^\top \mathbf{P}_{t+1} |\hat{\mathbf{z}}_m^{(t+1)}|^4, 2c\hat{\mathbf{z}}_m^{(t+1)}, \mathbf{x}_j^{(t)} - \hat{\mathbf{z}}_m^{(t+1)} \rangle = \frac{4c \cdot O(n^{-2} + \kappa)}{n_{t+1}} = O(n^{-2-\epsilon/4}).$$

Finally for Eq. (14), using Cauchy-Schwarz we have

$$\begin{aligned}
\frac{1}{B} \langle \mathbf{P}_{t+1}^\top \mathbf{P}_{t+1} |\hat{\mathbf{z}}_m^{(t+1)}|^3 \rangle &= \frac{1}{B} \langle |(\hat{\mathbf{z}}_{m,[t+1]}^{(t+1)})^3| \rangle = \frac{1}{B} \sum_{i=1}^B |(\hat{\mathbf{z}}_{m,[t+1],i}^{(t+1)})^3| \\
&\leq \frac{1}{B} \left( \sum_{i=1}^B (\hat{\mathbf{z}}_{m,[t+1],i}^{(t+1)})^2 \right)^{1/2} \left( \sum_{i=1}^B (\hat{\mathbf{z}}_{m,[t+1],i}^{(t+1)})^4 \right)^{1/2} \\
&= \frac{1}{B} O(Bn^{-1})^{1/2} O(Bn^{-1-\epsilon/4})^{1/2} \\
&= O(n^{-1-\epsilon/8}).
\end{aligned}$$

By the definition of  $\mathbf{P}_{t+1}$ , we get

$$\begin{aligned}
&\frac{1}{n_{t+1} B} \langle \mathbf{P}_{t+1}^\top (\mathbf{P}_{t+1} \phi(\hat{\mathbf{z}}_m^{(t+1)}) - \mathbf{b}_m), O(|\hat{\mathbf{z}}_m^{(t+1)}|^3), \mathbf{x}_j^{(t)} - \hat{\mathbf{z}}_m^{(t+1)} \rangle \\
&= \frac{1}{n_{t+1} B} \langle \phi(\hat{\mathbf{z}}_m^{(t+1)}) - \mathbf{P}_{t+1}^\top \mathbf{b}_m, O(\mathbf{P}_{t+1}^\top \mathbf{P}_{t+1} |\hat{\mathbf{z}}_m^{(t+1)}|^3), \mathbf{x}_j^{(t)} - \hat{\mathbf{z}}_m^{(t+1)} \rangle \\
&= \frac{4}{n_{t+1} B} O \left( \langle \mathbf{P}_{t+1}^\top \mathbf{P}_{t+1} |\hat{\mathbf{z}}_m^{(t+1)}|^3 \rangle \right) \\
&= O(n^{-2-\epsilon/8}).
\end{aligned}$$

Combining all terms from (11) to (14), for any  $j \in [n_{t+1}]$ , we get

$$\frac{\partial \mathcal{L}^{(t+1)}}{\partial w_{j,m}^{(t+1)}} = -\frac{2c}{n_{t+1}^2} \mathbb{1}(p[j] = m) + O(n^{-2-\epsilon/8})$$

**Case 2:**  $m > n_{t+2}$ . Under per-block gating,  $g_m^{(t+1)} = 0$ . The gated connection update at position  $m$  becomes

$$\mathbf{x}_{m,[t+2]}^{(t+1)} = \mathbf{x}_{m,[t+2]}^{(t)} + (1 - g_m^{(t+1)}) \mathbf{x}_{m,[t+1]}^{(t)} + g_m^{(t+1)} \phi(\hat{\mathbf{z}}_m^{(t+1)}) = \mathbf{x}_{m,[t+2]}^{(t)} + \mathbf{x}_{m,[t+1]}^{(t)},$$

which does not depend on  $\hat{\mathbf{z}}_m^{(t+1)}$  and hence not on  $\mathbf{w}_m^{(t+1)}$ . Therefore,  $w_{j,m}^{(t+1)}$  is absent from the loss  $\mathcal{L}^{(t+1)}$  entirely, giving

$$\frac{\partial \mathcal{L}^{(t+1)}}{\partial w_{j,m}^{(t+1)}} = 0$$

identically. After quantization,  $w_{j,m}^{(t+1)}$  remains zero.

**Concentration of attention scores at  $m \in [n_{t+1} + 1, n_{t+2}]$ .** Similar to Lemma 7, we choose a single stage-wise learning rate to ensure the non-child noise is rounded to zero using quantization,

$$\eta_{t+1} := \frac{K_n n_{t+1}^2}{2c}.$$

where  $K_n = \lceil n^{\epsilon/16} \rceil$  and where  $c > 0$  is the link function constant from Definition 2. Equivalently, the update for  $m \in [n_{t+1} + 1, n_{t+2}]$  is

$$w_{j,m}^{(t+1)}(t+1) = q\left(-\eta_{t+1} \tilde{\nabla}_{w_{j,m}^{(t+1)}} \mathcal{L}^{(t+1)}\right). \quad (15)$$

Using the gradient expansion,

$$-\tilde{\nabla}_{w_{j,m}^{(t+1)}} \mathcal{L}^{(t+1)} = \frac{2c}{n_{t+1}^2} \mathbb{1}(p[j] = m) + R_{j,m},$$

where the noise term satisfies

$$|R_{j,m}| \leq C_{\nabla} n^{-2-\epsilon/8}$$

uniformly over  $j \in [n_{t+1}]$  and  $m \in [n_{t+1} + 1, n_{t+2}]$ , we obtain

$$w_{j,m}^{(t+1)}(t+1) = q(K_n \mathbb{1}(p[j] = m) + \Delta_{j,m}), \quad (16)$$

where

$$\Delta_{j,m} := \eta_{t+1} R_{j,m}.$$

Since  $n_{t+1} \leq 2n$  on the trainable range and  $K_n \leq 2n^{\epsilon/16}$  for all sufficiently large  $n$ , we have

$$|\Delta_{j,m}| \leq \frac{K_n n_{t+1}^2}{2c} C_{\nabla} n^{-2-\epsilon/8} \leq C'_{\nabla} n^{-\epsilon/16},$$

for a constant  $C'_{\nabla} > 0$ . Hence

$$|\Delta_{j,m}| < \frac{1}{2}$$

for all sufficiently large  $n$ .

*Non-child indices.* For  $j \notin \{c_1[m], c_2[m]\}$ , the indicator  $\mathbb{1}(p[j] = m)$  vanishes. Therefore

$$w_{j,m}^{(t+1)}(t+1) = q(\Delta_{j,m}) = 0.$$

*Children indices.* For  $j \in \{c_1[m], c_2[m]\}$ , we have  $\mathbb{1}(p[j] = m) = 1$ . Since  $K_n \in \mathbb{Z}$  and  $|\Delta_{j,m}| < 1/2$ ,

$$w_{j,m}^{(t+1)}(t+1) = q(K_n + \Delta_{j,m}) = K_n.$$

Thus

$$w_{c_1[m],m}^{(t+1)}(t+1) = w_{c_2[m],m}^{(t+1)}(t+1) = K_n,$$

while all non-child logits are zero.

*Softmax concentration.* The total softmax mass on non-child indices is bounded by

$$\sum_{j \notin \{c_1[m], c_2[m]\}} \sigma_j(\mathbf{w}_m^{(t+1)}) \leq \frac{n}{2 \exp(K_n)} \leq n \exp(-K_n) \leq \exp(-Cn^{\epsilon/16})$$

for some constant  $C > 0$  and all sufficiently large  $n$ . Since the two child logits are exactly equal, the two children receive the same softmax weight. Therefore

$$\frac{1 - \exp(-Cn^{\epsilon/16})}{2} \leq \sigma_{c_1[m]}(\mathbf{w}_m^{(t+1)}) = \sigma_{c_2[m]}(\mathbf{w}_m^{(t+1)}) \leq \frac{1}{2}.$$

**Evaluating the forward pass.** To bound the prediction loss, we define the cumulative approximation error after stage  $t$  as

$$\epsilon_t := \max_{1 \leq s \leq t} \max_{m \in [n_s+1, n_{s+1}]} \|\mathbf{x}_{m, [s+1]}^{(s)} - \mathbf{b}_m\|_\infty, \quad \epsilon_0 := 0.$$

By construction,  $\epsilon_t$  is non-decreasing in  $t$  and bounds the error at every CoT position produced by layers  $1, \dots, t$ . In particular, for any  $m \in [n_{t+1} + 1, n_{t+2}]$ , the two children  $c_1[m], c_2[m]$  both lie at levels  $\leq t + 1$ , so they were produced by some layer  $s \leq t$  and satisfy

$$\|\mathbf{x}_{c_1[m], [t+1]}^{(t)} - \mathbf{b}_{c_1[m]}\|_\infty, \quad \|\mathbf{x}_{c_2[m], [t+1]}^{(t)} - \mathbf{b}_{c_2[m]}\|_\infty \leq \epsilon_t.$$

and for the intermediate state  $\hat{\mathbf{z}}_{m, [t+1]}^{(t+1)}$  we have

$$\begin{aligned} & \left\| \hat{\mathbf{z}}_{m, [t+1]}^{(t+1)} - \frac{\mathbf{b}_{c_1[m]} + \mathbf{b}_{c_2[m]}}{2} \right\|_\infty \\ & \leq \left\| \hat{\mathbf{z}}_{m, [t+1]}^{(t+1)} - \frac{\mathbf{x}_{c_1[m], [t+1]}^{(t)} + \mathbf{x}_{c_2[m], [t+1]}^{(t)}}{2} \right\|_\infty + \epsilon_t \\ & \leq \sum_{p[j] \neq m} \sigma_j(\mathbf{w}_m^{(t+1)}) + \left| \sigma_{c_1[m]}(\mathbf{w}_m^{(t+1)}) - \frac{1}{2} \right| + \left| \sigma_{c_2[m]}(\mathbf{w}_m^{(t+1)}) - \frac{1}{2} \right| + \epsilon_t \\ & \leq 2 \exp(-Cn^{\epsilon/16}) + \epsilon_t. \end{aligned} \tag{17}$$

Therefore, using the Taylor expansion of  $\phi$ , every newly produced position at stage  $t + 1$  satisfies

$$\begin{aligned} \|\mathbf{x}_{m, [t+2]}^{(t+1)} - \mathbf{b}_m\|_\infty &= \left\| \phi(\hat{\mathbf{z}}_{m, [t+1]}^{(t+1)}) - \phi\left(\frac{\mathbf{b}_{c_1[m]} + \mathbf{b}_{c_2[m]}}{2}\right) \right\|_\infty \\ &\leq C_2 (2 \exp(-Cn^{\epsilon/16}) + \epsilon_t)^2, \end{aligned}$$

for some constant  $C_2$  depending on  $\phi$  only. Combined with the cumulative max, this gives the recursion

$$\epsilon_{t+1} \leq \max\left\{ \epsilon_t, C_2 (2 \exp(-Cn^{\epsilon/16}) + \epsilon_t)^2 \right\}.$$

We inductively show that  $\epsilon_t \leq \delta := \exp(-Cn^{\epsilon/16})$  for all  $t$ . The base case  $\epsilon_1 \leq \delta$  holds by Lemma 7. Assume  $\epsilon_t \leq \delta$ . The first argument of the max is at most  $\delta$  by hypothesis, and the second is bounded by

$$C_2 (2\delta + \delta)^2 = 9C_2 \delta^2.$$

To conclude  $\epsilon_{t+1} \leq \delta$ , it suffices that  $9C_2\delta \leq 1$ , which holds for all sufficiently large  $n$  since  $\delta = \exp(-Cn^{\epsilon/16})$  decays faster than any polynomial. Thus  $\epsilon_t \leq \delta$  for all  $t \leq L = \log_2 k$  by induction. In particular, since position  $m = T$  at the final stage  $L$  is included in the cumulative max, we conclude

$$\|\mathbf{x}_{T,[L+1]}^{(L)} - \mathbf{b}_T\|_\infty = \|\hat{f}(\mathbf{D}_{\text{test}}) - \mathbf{y}_{\text{test}}\|_\infty \leq \exp(-Cn^{\epsilon/16}).$$

□

We are now ready to combine the lemmas of this section into a proof of Theorem 1.

*Proof of Theorem 1.* We prove by induction on  $t \in \{1, \dots, L\}$  that after stage  $t$ , layers  $1, \dots, t$  are well-trained (Definition 4) and  $\mathbf{W}^{(\ell)}(t) = 0$  for all  $\ell \geq t + 1$ .

**Base case ( $t = 1$ ).** At initialization,  $\mathbf{W}^{(\ell)}(0) = 0$  for all  $\ell \in [L]$  (Algorithm 1). The stage-1 update modifies only  $\mathbf{W}^{(1)}$ , leaving  $\mathbf{W}^{(\ell)}(1) = 0$  for all  $\ell \geq 2$ . By Lemma 7, with probability  $1 - \exp(-n^{\epsilon/2})$  over the stage-1 batch, layer 1 is well-trained.

**Inductive step ( $t \rightarrow t + 1$ ).** Assume that after stage  $t$ , layers  $1, \dots, t$  are well-trained and  $\mathbf{W}^{(\ell)}(t) = 0$  for all  $\ell \geq t + 1$ . We show the same holds at stage  $t + 1$ .

The inductive hypothesis verifies the assumption of Lemma 10. Applying it, for every  $\ell' \leq t$ ,  $m \in [n_{\ell'} + 1, n_{\ell'+1}]$ , and  $j \in [n_{\ell'}]$ ,

$$\left| \frac{\partial \mathcal{L}^{(t+1)}}{\partial w_{j,m}^{(\ell')}} \right| \leq O(\exp(-Cn^{\epsilon/16})),$$

and the quantized stage- $(t + 1)$  update leaves  $w_{j,m}^{(\ell')}(t + 1) = w_{j,m}^{(\ell')}(t)$ . Hence layers  $1, \dots, t$  remain well-trained after stage  $t + 1$ . The inductive hypothesis also verifies the assumption of Lemma 9. Applying it, with probability  $1 - \exp(-n^{\epsilon/2})$  over the fresh stage- $(t + 1)$  batch, layer  $t + 1$  is well-trained. The stage- $(t + 1)$  update modifies only  $\mathbf{W}^{(t+1)}$ , so  $\mathbf{W}^{(\ell)}(t + 1) = \mathbf{W}^{(\ell)}(t) = 0$  for all  $\ell \geq t + 2$ . This completes the inductive step.

**Union bound and conclusion.** Each stage's well-trainedness conclusion holds with probability  $1 - \exp(-n^{\epsilon/2})$  over its fresh batch, and the  $L = \log_2 k$  batches are independent. By a union bound, with probability at least

$$1 - L \exp(-n^{\epsilon/2}) = 1 - \exp(-\Omega(n^{\epsilon/2}))$$

(using  $L = O(\log n)$ ), every layer  $\ell \in [L]$  is well-trained after stage  $L$ . By Definition 4 applied at layer  $L$  and position  $m = T$  (which lies in  $[n_L + 1, n_{L+1}]$  since  $n_{L+1} = T$ ),

$$\|\mathbf{x}_{T,[L+1]}^{(L)} - \mathbf{b}_T\|_\infty \leq \exp(-Cn^{\epsilon/16}).$$

By Lemma 2 applied at  $\beta = T$ ,  $\ell = L$ , the test-time output at position  $T$  satisfies

$$f_{\hat{\theta}}^L(\mathbf{D}_{\text{test}})_T = \Psi_L^\top \mathcal{T}_{\hat{\theta}}(\mathbf{D}_{\text{test}})_T = \mathbf{x}_{T,[L+1]}^{(L)},$$

and the target is  $\mathbf{y}_{\text{test}} = \mathbf{b}_T$ . Therefore

$$\|f_{\hat{\theta}}^L(\mathbf{D}_{\text{test}})_T - \mathbf{y}_{\text{test}}\|_\infty \leq \exp(-Cn^{\epsilon/16}) = \exp(-\Omega(n^{\epsilon/16})),$$

which establishes the theorem. □

## C.6 Gradient Upper Bound for Trained Layers

**Lemma 10** (Frozen gradient). *Fix any  $t \in \{1, \dots, L-1\}$ . Suppose layers  $1, \dots, t$  are well-trained (Definition 4) and  $\mathbf{W}^{(\ell)}(t) = 0$  for all  $\ell \geq t+1$ . Then during one stage- $(t+1)$  gradient step, for any  $\ell' \leq t$ , any  $m \in [n_{\ell'} + 1, n_{\ell'+1}]$ , and any  $j \in [n_{\ell'}]$ ,*

$$\left| \frac{\partial \mathcal{L}^{(t+1)}}{\partial w_{j,m}^{(\ell')}} \right| \leq O(\exp(-Cn^{\epsilon/16})).$$

Consequently, with the stage-wise learning rate  $\eta_{t+1} = \Theta(K_n n_{t+1}^2)$  (where  $K_n := \lceil n^{\epsilon/16} \rceil$ ), the weights in all previously trained layers remain unchanged after quantization:

$$w_{j,m}^{(\ell')}(t+1) = w_{j,m}^{(\ell')}(t) \quad \text{for all } \ell' \leq t, m \in [n_{\ell'} + 1, n_{\ell'+1}], j \in [n_{\ell'}].$$

*Proof.* Throughout, fix  $\ell' \leq t$  and a parameter  $w_{j,m}^{(\ell')}$  with  $n_{\ell'} + 1 \leq m \leq n_{\ell'+1}$  and  $1 \leq j \leq n_{\ell'}$ . Let  $L_\phi := \|\phi'\|_\infty$ .

**Step 1: Vanishing of  $\phi'$  at well-trained positions.** Recall from Lemma 9 that, by the assumption on the softmax weights, for any  $\ell'' \leq t$  and  $n_{\ell''} + 1 \leq \alpha \leq n_{\ell''+1}$ ,

$$\left\| \hat{\mathbf{z}}_{\alpha, [\ell'']}^{(\ell'')} - \frac{\mathbf{b}_{c_1[\alpha]} + \mathbf{b}_{c_2[\alpha]}}{2} \right\|_\infty \leq (2n-1) \exp(-Cn^{\epsilon/16}). \quad (18)$$

By Definition 2,  $\phi'(0) = \phi'(\pm 1) = 0$ , and the local Taylor expansions  $\phi'(t) = 2ct + O(|t|^3)$  near 0 and  $\phi'(t) = O(1 - |t|)$  near  $\pm 1$  yield a constant  $C_\phi > 0$  such that

$$|\phi'(t)| \leq C_\phi |t - z_i^*| \quad \text{whenever } z_i^* \in \{-1, 0, +1\} \text{ is the nearest zero of } \phi' \text{ to } t. \quad (19)$$

Since  $\mathbf{b}_{c_1[\alpha]}, \mathbf{b}_{c_2[\alpha]} \in \{-1, +1\}^B$ , their average lies coordinate-wise in  $\{-1, 0, +1\}$ . Applying (19) coordinate-wise with (18),

$$\|\phi'(\hat{\mathbf{z}}_{\alpha, [\ell'']}^{(\ell'')})\|_\infty \leq C_\phi \left\| \hat{\mathbf{z}}_{\alpha, [\ell'']}^{(\ell'')} - \frac{\mathbf{b}_{c_1[\alpha]} + \mathbf{b}_{c_2[\alpha]}}{2} \right\|_\infty \leq O(\exp(-Cn^{\epsilon/16})).$$

**Step 2: Per-node sensitivity under the well-trained hypothesis.** Recall the per-node sensitivity defined in Lemma 3:

$$\xi_{j,m,\ell'}^{(\ell)} := \max_{\beta: h[\beta] \leq \ell+1} \left\| \frac{\partial \mathbf{x}_{\beta, [\ell+1]}^{(\ell)}}{\partial w_{j,m}^{(\ell')}} \right\|_\infty.$$

We claim that for all  $\ell' \leq \ell \leq t$ ,

$$\xi_{j,m,\ell'}^{(\ell)} \leq O(\exp(-Cn^{\epsilon/16})).$$

*Base case  $\ell = \ell'$ .* By Corollary 1, only  $\beta$  with active layer equal to  $\ell'$ , i.e.,  $\nu := h[\beta] = \ell' + 1$ , contribute. For such  $\beta$ ,

$$\frac{\partial \mathbf{x}_{\beta, [\ell'+1]}^{(\ell')}}{\partial w_{j,m}^{(\ell')}} = \phi'(\hat{\mathbf{z}}_{\beta, [\ell']}^{(\ell')}) \odot \frac{\partial \hat{\mathbf{z}}_{\beta, [\ell']}^{(\ell')}}{\partial w_{j,m}^{(\ell')}},$$

and the parameter  $w_{j,m}^{(\ell')}$  enters only through the softmax at query position  $\beta = m$ , giving

$$\frac{\partial \hat{\mathbf{z}}_{m,[\ell']}^{(\ell')}}{\partial w_{j,m}^{(\ell')}} = \sigma_j(\mathbf{w}_m^{(\ell')}) (\mathbf{x}_{j,[\ell']}^{(\ell'-1)} - \hat{\mathbf{z}}_{m,[\ell']}^{(\ell')}).$$

Since  $\mathbf{x}_{j,[\ell']}^{(\ell'-1)}, \hat{\mathbf{z}}_{m,[\ell']}^{(\ell')} \in [-1, 1]^B$ , their difference lies in  $[-2, 2]^B$ . Combining with Step 1,

$$\xi_{j,m,\ell'}^{(\ell')} \leq 2 \|\phi'(\hat{\mathbf{z}}_{m,[\ell']}^{(\ell')})\|_\infty \cdot \sigma_j(\mathbf{w}_m^{(\ell')}) \leq O(\exp(-Cn^{\epsilon/16})).$$

*Inductive step  $\ell \Rightarrow \ell + 1$  ( $\ell + 1 \leq t$ ).* Take  $\beta$  with  $h[\beta] \leq \ell + 2$ .

*Sub-case A:*  $h[\beta] \leq \ell + 1$ . By Lemma 2,  $\mathbf{x}_{\beta,[\ell+2]}^{(\ell+1)} = \mathbf{x}_{\beta,[\ell+1]}^{(\ell)}$ , so the derivative is bounded by  $\xi_{j,m,\ell'}^{(\ell)}$ .

*Sub-case B:*  $h[\beta] = \ell + 2$ . Corollary 1 gives

$$\frac{\partial \mathbf{x}_{\beta,[\ell+2]}^{(\ell+1)}}{\partial w_{j,m}^{(\ell')}} = \phi'(\hat{\mathbf{z}}_{\beta,[\ell+1]}^{(\ell+1)}) \odot \frac{\partial \hat{\mathbf{z}}_{\beta,[\ell+1]}^{(\ell+1)}}{\partial w_{j,m}^{(\ell')}}.$$

Since  $\ell + 1 \leq t$ , Step 1 yields  $\|\phi'(\hat{\mathbf{z}}_{\beta,[\ell+1]}^{(\ell+1)})\|_\infty \leq O(\exp(-Cn^{\epsilon/16}))$ . Differentiation passes through the softmax (since  $\ell' \leq \ell < \ell + 1$ ):

$$\frac{\partial \hat{\mathbf{z}}_{\beta,[\ell+1]}^{(\ell+1)}}{\partial w_{j,m}^{(\ell')}} = \sum_{\gamma} \sigma_{\gamma}(\mathbf{w}_{\beta}^{(\ell+1)}) \frac{\partial \mathbf{x}_{\gamma,[\ell+1]}^{(\ell)}}{\partial w_{j,m}^{(\ell')}},$$

each summand bounded by  $\xi_{j,m,\ell'}^{(\ell)}$  in  $\infty$ -norm and the softmax weights summing to 1. Hence

$$\left\| \frac{\partial \mathbf{x}_{\beta,[\ell+2]}^{(\ell+1)}}{\partial w_{j,m}^{(\ell')}} \right\|_\infty \leq O(\exp(-Cn^{\epsilon/16})) \cdot \xi_{j,m,\ell'}^{(\ell)}.$$

*Combining sub-cases.*

$$\xi_{j,m,\ell'}^{(\ell+1)} \leq \xi_{j,m,\ell'}^{(\ell)} \leq O(\exp(-Cn^{\epsilon/16})),$$

where the second inequality is the inductive hypothesis.

**Step 3: Bounding the layer- $(t + 1)$  output gradient.** For any  $\alpha \in [n_{t+1} + 1, T]$ , the softmax weights at layer  $t + 1$  are independent of  $w_{j,m}^{(\ell')}$  as layer  $t + 1$  has not yet been trained. By chain rule,

$$\frac{\partial \phi(\hat{\mathbf{z}}_{\alpha,[t+1]}^{(t+1)})}{\partial w_{j,m}^{(\ell')}} = \phi'(\hat{\mathbf{z}}_{\alpha,[t+1]}^{(t+1)}) \odot \sum_{\gamma} \sigma_{\gamma}(\mathbf{w}_{\alpha}^{(t+1)}) \cdot \frac{\partial \mathbf{x}_{\gamma,[t+1]}^{(t)}}{\partial w_{j,m}^{(\ell')}}.$$

Bounding by  $\|\phi'\|_\infty \leq L_\phi$ , summing softmax weights to 1, and using Step 2's bound  $\xi_{j,m,\ell'}^{(t)} \leq O(\exp(-Cn^{\epsilon/16}))$ ,

$$\left\| \frac{\partial \phi(\hat{\mathbf{z}}_{\alpha,[t+1]}^{(t+1)})}{\partial w_{j,m}^{(\ell')}} \right\|_\infty \leq L_\phi \cdot \xi_{j,m,\ell'}^{(t)} \leq O(\exp(-Cn^{\epsilon/16})).$$

**Step 4: Pulling back through the loss.** The stage- $(t+1)$  loss reads

$$\mathcal{L}^{(t+1)}(\boldsymbol{\theta}) = \frac{1}{2B} \sum_{\alpha=n_{t+1}+1}^T \|\mathbf{P}_{t+1} \left( g_{\alpha}^{(t+1)} \phi(\hat{\mathbf{z}}_{\alpha}^{(t+1)}) + (1 - g_{\alpha}^{(t+1)}) \mathbf{x}_{\alpha}^{(t)} \right) - \mathbf{b}_{\alpha}\|^2.$$

Splitting the sum by the gating rule Eq. (2),  $g_{\alpha}^{(t+1)} = 1$  for  $\alpha \in [n_{t+1} + 1, n_{t+2}]$  and  $g_{\alpha}^{(t+1)} = 0$  for  $\alpha > n_{t+2}$  and differentiating,

$$\begin{aligned} & \left| \frac{\partial \mathcal{L}^{(t+1)}}{\partial w_{j,m}^{(\ell')}} \right| \\ &= \frac{1}{B} \left| \sum_{\alpha=n_{t+1}+1}^{n_{t+2}} (\mathbf{P}_{t+1} \phi(\hat{\mathbf{z}}_{\alpha}^{(t+1)}) - \mathbf{b}_{\alpha})^{\top} \frac{\partial \mathbf{P}_{t+1} \phi(\hat{\mathbf{z}}_{\alpha}^{(t+1)})}{\partial w_{j,m}^{(\ell')}} + \sum_{\alpha=n_{t+2}+1}^T (\mathbf{P}_{t+1} \mathbf{x}_{\alpha}^{(t)} - \mathbf{b}_{\alpha})^{\top} \frac{\partial \mathbf{P}_{t+1} \mathbf{x}_{\alpha}^{(t)}}{\partial w_{j,m}^{(\ell')}} \right| \\ &\stackrel{(a)}{\leq} \sum_{\alpha=n_{t+1}+1}^{n_{t+2}} \frac{1}{B} \|\mathbf{P}_{t+1} \phi(\hat{\mathbf{z}}_{\alpha}^{(t+1)}) - \mathbf{b}_{\alpha}\|_1 \cdot \left\| \frac{\partial \phi(\hat{\mathbf{z}}_{\alpha, [t+1]}^{(t+1)})}{\partial w_{j,m}^{(\ell')}} \right\|_{\infty} \\ &\quad + \sum_{\alpha=n_{t+2}+1}^T \frac{1}{B} \|\mathbf{P}_{t+1} \mathbf{x}_{\alpha}^{(t)} - \mathbf{b}_{\alpha}\|_1 \cdot \left\| \frac{\partial \mathbf{x}_{\alpha, [t+1]}^{(t)}}{\partial w_{j,m}^{(\ell')}} \right\|_{\infty} \\ &\stackrel{(b)}{\leq} 2 \sum_{\alpha=n_{t+1}+1}^{n_{t+2}} \left\| \frac{\partial \phi(\hat{\mathbf{z}}_{\alpha, [t+1]}^{(t+1)})}{\partial w_{j,m}^{(\ell')}} \right\|_{\infty} + 2 \sum_{\alpha=n_{t+2}+1}^T \left\| \frac{\partial \mathbf{x}_{\alpha, [t+1]}^{(t)}}{\partial w_{j,m}^{(\ell')}} \right\|_{\infty} \\ &\stackrel{(c)}{\leq} O(\exp(-Cn^{\epsilon/16})), \end{aligned}$$

where (a) applies Hölder's inequality and uses that  $\mathbf{P}_{t+1}$  extracts block  $[t+1]$ , (b) uses  $\mathbf{P}_{t+1} \phi(\hat{\mathbf{z}}_{\alpha}^{(t+1)})$ ,  $\mathbf{P}_{t+1} \mathbf{x}_{\alpha}^{(t)}$ ,  $\mathbf{b}_{\alpha} \in [-1, 1]^B$ , and (c) bounds the first sum by Step 3 and the second sum by the fact that positions  $\alpha \geq n_{t+2} + 1$  has not been written by layer  $\ell' \in [t]$ . The factor of  $T \leq 2n$  from each sum is absorbed into the exponential.

**Step 5: Quantization freezes the weight.** With the stage-wise learning rate  $\eta_{t+1} = \Theta(K_n n_{t+1}^2)$  where  $K_n = \lceil n^{\epsilon/16} \rceil$ , the proposed update reads

$$\begin{aligned} w_{j,m}^{(\ell')}(t) - \eta_{t+1} \tilde{\nabla}_{w_{j,m}^{(\ell')}} \mathcal{L}^{(t+1)} &= w_{j,m}^{(\ell')}(t) + O(K_n n_{t+1}^2 \left( \exp(-Cn^{\epsilon/16}) + n^{-2-\epsilon/8} \right)) \\ &= w_{j,m}^{(\ell')}(t) + O(n^{-\epsilon/16}), \end{aligned}$$

which the nearest-integer operator  $q(\cdot)$  rounds back to  $w_{j,m}^{(\ell')}(t)$  for sufficiently large  $n$ .  $\square$